Deep learning predicts onset acceleration of 38 age-associated diseases from blood and body composition biomarkers in the UK Biobank

Mica Xu Ji[1*], Marjola Thanaj[1], Léna Nehale-Ezzine[2], Brandon Whitcher[1], E. Louise Thomas[1], Jimmy D. Bell[1]

[1*]Research Centre for Optimal Health, School of Life Sciences, University of Westminster, London, UK.
[2]Mila – Quebec AI Institute, Montreal, Canada.

*Corresponding author. E-mail: m.ji1@westminster.ac.uk

Abstract

A major challenge in multimorbid aging is understanding how diseases co-occur and identifying high-risk groups for accelerated disease development, but to date associations in the relative onset acceleration of disease diagnoses have not been used to characterise disease patterns. This study presents the development and evaluation of a neural network Cox model for predicting onset acceleration risk for age-associated conditions, using demographic, anthropomorphic, imaging and blood biomarker traits from 60,396 individuals and 218,530 outcome events from the UK Biobank. Risk prediction was evaluated with Harrell's concordance index (C-index). The model performed well on internal (C-index $\mathbf{0.6830 \pm 0.0902}$, $\boldsymbol{n = 8,931}$) and external (C-index $\mathbf{0.6461 \pm 0.1264}$, $\boldsymbol{n = 855}$) test sets, attaining C-index $\geq \mathbf{0.6}$ on 38 out of 47 (**80.9%**) conditions. Inclusion of body composition and blood biomarker input traits were independently important for predictive performance. Kaplan-Meier curves for predicted risk quartiles (log-rank $\boldsymbol{p \leq 1.16E-16}$) indicated robust stratification of individuals into high and low risk groups. Analysis of risk quartiles revealed cardiometabolic, vascular-neuropsychiatric, and digestive-neuropsychiatric disease clusters with strong statistically significant inter-correlated onset acceleration ($\boldsymbol{r \geq 0.6}$, $\boldsymbol{p \leq 3.46E-5}$), while 13 and 19 conditions were strongly associated with onset acceleration of all cause mortality and all cause morbidity respectively.

In prognostic survival analysis, the proportional hazards assumption was met (Schoenfeld residual $\boldsymbol{p > 0.05}$) in 435 out of 435 or 100% (1238 out of 1334 or 92.8%) of cases across outcomes, $\boldsymbol{aHR = 6.11 \pm 9.00}$ ($\boldsymbol{aHR = 3.67 \pm 5.78}$) with (without) Bonferroni correction. The neural architecture of OnsetNet was interpreted with saliency analysis and several significant body composition and blood biomarkers were identified. The results demonstrate that neural network survival models are able to estimate prognostically informative onset acceleration risk, which could be used to improve understanding of synchronicity in the onset of age-associated diseases and reprioritize patients based on disease-specific risk.

Keywords: multimorbidity, deep learning, healthy aging, UK Biobank

1 Introduction

As we age, the probability of developing more than one condition greatly increases [1]. Multimorbidity, which can be defined as co-occurrence of more than one condition in the same individual, is thus an important problem in aging societies [2, 3], being associated with lower quality of life [4], higher mortality risk [5], and greater usage of healthcare resources than healthy people or those with just one chronic condition [6, 7]. There is a high and increasing prevalence of multimorbidity in the general population, with elderly and socioeconomically deprived groups particularly at risk [1, 8–10]. Chowdhury et al. [11] determined that the global prevalence of multimorbidity was 37.2%, rising to 51.0% in people over 60 years old, while Nunes et al. [12] found that mortality risk of individuals with multimorbidity was 1.73 times greater than those without multimorbidity. Despite these concerns, healthcare delivery systems and quality evaluation remain focused on the treatment of single diseases [13, 14]. An important part of generating an evidence base for improvements in clinical practice is ascertaining patterns of disease and inter-disease associations beyond chance [15].

While epidemiological studies of multimorbidity vary widely in sample size, age settings and statistical methodology, there is a growing consensus that age-associated chronic diseases do not co-occur randomly but in associated fashion,

including conditions across the physical and mental health divide [1, 16]. A 2014 meta-review of 14 studies [15] identified cardiometabolic, neuropsychiatric-gastrointestinal, and musculoskeletal-vascular-neuropsychiatric-gastrointestinal co-occurrence clusters, while more recently [17] identified cardiometabolic, neuropsychiatric, and allergic disease co-occurrence clusters as being commonly reported among 41 studies. The majority of reviewed studies used agglomeration methods such as agglomerative hierarchical clustering and explanatory factor analysis to link diseases on the basis of co-occurrence in individuals, and were not restricted to age-associated conditions. While co-occurrence is important for characterising disease associations, another significant factor is age of disease onset [1]. For example, whether an individual develops cardiovascular disease or hearing loss may be less informative for their health status than age of onset, given that prevalence is estimated at 79-86% and 80.6% in those older than 80 and 85 respectively in the United States [18, 19]. The timing of disease onset has been shown to be informative for risk of secondary diagnoses; early onset cancer is associated with increased risk of cardiovascular disease and secondary cancers compared to later onset cancer [20, 21]. Accelerated biological age estimated using DNA methylation or phenotypic aging clocks has been associated with increased risk of mortality and adverse health outcomes compared to less accelerated biological age [22, 23]. A recent study on chronic diseases [24] found that certain lifestyle factors affected only age of onset and not odds of diagnosis for 10 cardiometabolic, autoimmune and respiratory conditions. Taken together, this suggests that the temporal dimension of multimorbidity may be important for characterising disease patterns.

The present study aims to determine (1) the extent to which onset acceleration risk of age-associated diseases can be accurately predicted from individual traits, and (2) how strongly early onset risk of one disease is associated with early onset risk of another disease beyond chance. To this end, Cox models were trained and evaluated for prediction of individual risk for early onset of diverse age-associated diseases. Using

data from 60,396 individuals in the UK Biobank imaging cohort [25], we trained a single multimodal neural network, OnsetNet, to predict time-to-event log-risk of the first diagnosis of 47 conditions with birth as temporal baseline, including two composite conditions of all-cause mortality and all-cause morbidity.

First, we evaluated performance of neural network models across disease conditions using C-index measured on internal center and external center held-out test sets, where model hyperparameters were selected by fivefold cross-validation and internal test and C-index ≥ 0.6 was considered acceptable prediction [26]. We compared performance of neural network models on eight different combinations of five input trait groups (demographic, anthropomorphic, summary body composition, spatial body composition, and blood biomarkers) totalling 43 input variables. We assessed performance differences between neural network and linear architectures to evaluate the benefit of using a neural network, which is state-of-the-art and may be a more appropriate choice where it is too simplistic to assume linearity of the log-risk function [27]. OnsetNet score quartiles were computed to illustrate within-disease heterogeneity across onset acceleration risk quartiles. Between-disease risk relationships were analysed by computing all-to-all correlations in OnsetNet risk quartiles between diseases, and clusters containing disease conditions with high inter-correlated onset acceleration risk were identified with agglomerative hierarchical clustering. We trained standard prognostic linear adjusted Cox models (baseline as measurement time, pre-existing diagnoses excluded) with OnsetNet score as an input trait, yielding adjusted hazard ratios across disease pairs. The proportional hazards assumption was tested by examination of Schoenfeld residuals. Finally, the model was analysed with gradient-based saliency to infer relative importance of individual biomarkers and to assess for biological validity of learned associations between biomarkers and disease risk.

OnsetNet's output is interpretable as a metric of accelerated biological aging, given that accelerated biological age can be characterized as event acceleration risk of

age-associated disease from birth [28]. While the present study is purely associative, OnsetNet's ability to stratify individuals into high and low risk groups may be useful for clinical settings, where important problems include early identification of high-risk individuals in order to effectively reduce disease burden on the general population [29] and characterising within-disease heterogeneity due to diversity in pathology [30, 31].

2 Methods

2.1 Study participants

This study was a secondary analysis of longitudinal data from the UK Biobank resource [32] under application number 44584. Data was obtained from the UK Biobank imaging cohort [33] for 60,396 individuals who were initially assessed between April 2007 and October 2010 and had outcomes recorded up to November 30th 2022 (follow-up 13.9 ± 0.819 years, min 12.2 years, max 15.6 years). Eligible individuals had full records of all covariates (29,873 male, 30,523 female, age at imaging 66.2 ± 8.01 years). Where multiple measurements were made, the latest measurement for each individual was taken. Data was split into a training and validation dataset (train-val) containing individuals assessed at Cheadle, Reading, Newcastle and unspecified centers (24,984 male, 25,626 female, age at imaging 66.2 ± 8.00 years), an internal test set containing individuals assessed at train-val centers (4,455 male, 4,476 female, age at imaging 66.0 ± 8.10 years), and an external test set contained individuals assessed at the Bristol center (434 male, 421 female, age at imaging 67.9 ± 7.54 years).

2.2 Covariates

Input variables were selected based on risk factors identified in literature review and were separated into 5 groups. Demographic ("demog") contained sex, race, education level, and Townsend deprivation index. Basic body ("bb") contained weight, height, body mass index (BMI), waist circumference, grip strength, systolic blood pressure,

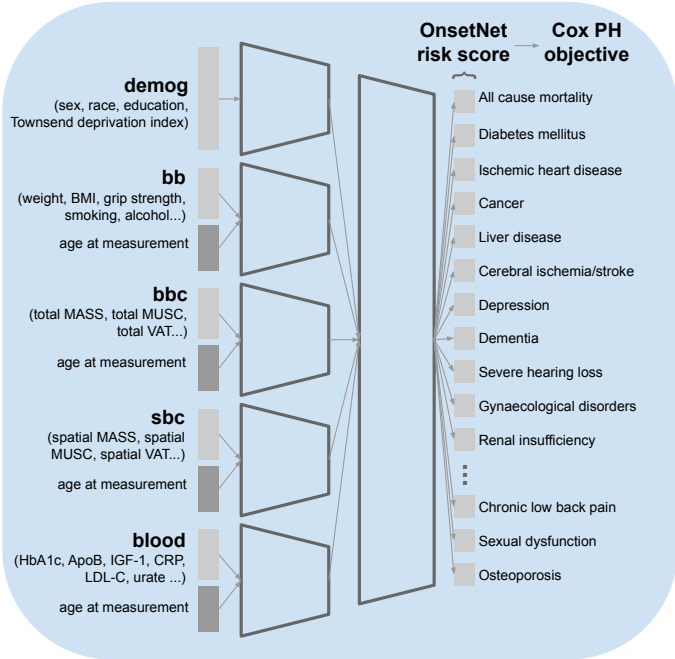

Fig. 1: Architecture of OnsetNet, a neural network Cox model trained to predict onset acceleration as log-risk of first incidence of 47 disease conditions from individual traits, using birth as temporal baseline. Abbreviations: body mass index (BMI), body mass (MASS), muscle (MUSC), visceral adipose tissue (VAT), glycated haemoglobin (HbA1c), apolipoprotein B (ApoB), insulin-like growth factor 1 (IGF-1), c-reactive protein (CRP), low-density lipoprotein cholesterol (LDL-C).

alcohol consumption, and smoking history. Basic body composition computed from neck-to-knee magnetic resonance imaging scans ("bbc") contained total mass (MASS), total subcutaneous adipose tissue volume (SAT), total muscle volume (MUSC), total visceral adipose tissue volume (VAT), and total thigh intramuscular and intermuscular adipose tissue mass (TMAT). Multidimensional spatial body composition ("sbc") contained MASS, SAT, MUSC, VAT, and TMAT measured along 370 slices across the vertical height dimension. Blood-based biomarkers ("blood") contained low-density lipoprotein cholesterol (LDL-C), triglycerides, apolipoprotein A (ApoA), apolipoprotein B (ApoB), cholesterol, high-density lipoprotein cholesterol (HDL-C), glucose, glycated haemoglobin (HbA1c), insulin-like growth factor 1 (IGF-1), urate, urea, total

protein, alanine aminotransferase (ALT), albumin (ALB), alkaline phosphatase (ALP), aspartate aminotransferase (AST), c-reactive protein (CRP), calcium (Ca), creatinine, cystatin C, gamma glutamyltransferase (GGT), phosphate, sex hormone binding globulin (SHBG), total bilirubin, and vitamin D.

For non-demographic variables, age at trait measurement was provided as an additional input variable with the measurement (Figure 1). Continuous input variables were scaled to zero mean and unit standard deviation using statistics from the train-val dataset, and discrete input variables were represented with one-hot encodings. Body composition variables were computed by automated segmentation of MRI instances by a previously published deep learning system that was used to produce publicly available UK Biobank body composition variables [34–37]. In brief, UNet [38] based deep learning models were trained to segment body composition tissues from UKBiobank neck-to-knee Dixon acquisitions using manual annotations. The UKBiobank protocol utilized the Siemens Aera 1.5T scanner (Syngo MR D13) and is detailed in [33].

Outcomes for 47 age-related conditions were chosen using literature on aging and multimorbidity [39, 40]. We obtained date of first occurrence for 45 non-composite disease categories defined by ICD10 codes (Appendix A.4) from the UK Biobank first occurrence register, which incorporates primary care, hospital inpatient, death register and self-reported records. Date of death was taken from the death register and date for all-cause morbidity was taken as first occurrence date for any of the 45 non-composite disease categories.

2.3 Deep learning estimation of onset acceleration risk

Neural network models trained to predict onset acceleration risk consisted of separate encoders per trait group each producing a feature vector of fixed length $k \in \{128, 256, 512\}$, followed by feature concatenation and a shared predictor head

with one scalar output for each disease condition (Figure 1). Neural networks had an average of $2.31E6 \pm 1.00E6$ parameters (min 8.54E5, max 4.92E6, Appendix B).

Fivefold cross-validation was used to train models on the train-val dataset by optimizing objective $l(\theta)$, the Cox proportional hazard (Cox PH) partial log-likelihood objective function with weight decay regularization [41] over 47 disease conditions $d \in \mathcal{D}$:

$$g^d(\theta) = -\frac{1}{N_{E^d=1}} \sum_{i:E_i^d=1} \left(h_\theta^d(x_i) - \log \sum_{j \in \mathcal{R}^d(T_i^d)} e^{h_\theta^d(x_j)} \right),$$
$$l(\theta) = \frac{1}{|\mathcal{D}|} \sum_{d \in \mathcal{D}} g^d(\theta) + \lambda \|\theta\|_2^2,$$

where θ are model parameters, λ is the weight decay coefficient, x_i are input traits for individual i, log-risk $h_\theta^d(x_i)$ is the scalar output of the model for disease condition d and individual i, E^d is the censoring vector for d where $E_i^d = 1$ (uncensored) if individual with index i received a diagnosed for d and $E_i^d = 0$ (censored) otherwise. $N_{E^d=1}$ is the number of uncensored individuals for d. Birth was used as temporal baseline and time to event was measured in years (Figure 2). T_i^d is age at first diagnosis for individual i with a diagnosis of d and otherwise age at censor date (November 30th 2022), risk set $\mathcal{R}^d(t) = \{i : T_i^d \geq t\}$ is the set of individuals undiagnosed with d at age t.

To evaluate performance, test sets were unseen during model selection of neural network Cox models and linear Cox comparison baselines. Hyperparameter values (λ, k, learning rate, dropout rate) for each input trait group combination were chosen by average validation fold C-index. Computation of C-index

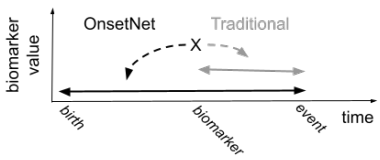

Fig. 2: Cox models commonly predict risk of event earliness from measurement baseline while OnsetNet models event earliness from birth.

was batched with batch size of 2048 for tractability [27]. Neural networks were implemented in Python with GPU-accelerated PyTorch 2.4.1 and linear models in R 4.1.2. The code will be made available upon publication.

2.4 Statistical analysis

To investigate onset acceleration risk correlation between conditions, Pearson's r was computed between OnsetNet score quartiles $q \in [1, 4]$ for all pairs of conditions with internal test C-index performance ≥ 0.6. Correlation of $r \geq 0.6$ was considered strong and $p \leq 3.46E-5$ was considered significant. Using the all-pairs correlation matrix, a clustering dendrogram was computed using unweighted pair group method with arithmetic mean (UPGMA) hierarchical agglomerative clustering for the linkage function (SciPy *cluster.hierarchy.linkage*) with cosine distance between correlation vectors as the clustering metric. Statin users (12,157 out of 60,396 in the study cohort reporting statin medication usage in verbal interview) were removed, and sensitivity analyses were conducted for removal of Bonferroni correction and inclusion of statin users.

To evaluate the prognostic ability of onset acceleration scores, a prognostic Cox model was trained for each pair of disease conditions (A, B), with OnsetNet risk quartile for condition A as input and individual log-risk of time-to-event for first occurrence of condition B as output. Baseline time was taken as imaging assessment time, corresponding to the latest date across input trait measurements, outcome events were within 10 years of baseline, individuals with pre-existing diagnoses were excluded, and time-to-event was measured in months. Demographic traits were included as input covariates for primary adjustment of hazard ratios, and secondary adjustment for both demographic and basic body traits was also performed to test for sensitivity. 6 outcome conditions with greater than 75% allocation to either sex (female: gynecological problems, thyroid diseases, osteoporosis; male: prostatic hyperplasia, hyperuricemia/gout, sexual dysfunction) were trained for the dominant sex only. Outcome events

for 3 conditions with fewer than 50 uncensored individuals after removal of pre-imaging diagnoses were removed (hemorrhoids, Parkinson's disease, and somatoform disorders).

Two-tailed tests were used to compute p-values and Bonferroni corrections were made at $p = 0.05$ level. The study adhered to the EQUATOR TRIPOD+ AI [42] guidelines for transparent reporting of an AI multivariable prediction model and STROBE [43] guidelines for reports of observational studies. Completed checklists are given in Appendix D.

3 Results

3.1 Predictive performance

A summary of participant characteristics for training and test datasets is given in Table 1. Eight different combinations of trait group inputs were evaluated for the neural network OnsetNet architecture and compared to a linear architecture (Table 2). High-dimensional spatial body composition was utilized for neural network models but not linear models due to correlation in body composition along the height dimension. The OnsetNet full traits model (demog+bb+bbc+sbc+blood) attained the highest internal test C-index ($0.6830 \pm 9.02E-2$), highest combined internal and external test C-index ($0.6647 \pm 1.11E-1$), and highest validation C-index ($0.6856 \pm 9.08E-1$) on average over conditions and cross-validation data folds. On the external test set, OnsetNet demog+bb+bbc+blood ($0.6472 \pm 1.23E-1$) performed best on C-index, followed by OnsetNet full traits ($0.6461 \pm 1.26E-1$). While performance differences between top OnsetNet models and the linear model were not statistically significant by estimated p-value, larger differences between models were statistically significant (Table 2, Table C10), and the linear model was consistently outperformed by neural networks on all metrics. Within specific conditions, diabetes mellitus non-T1 ($0.940 \pm$

Table 1: Characteristics of UK Biobank participants used for the present study. p-values were computed with two-tailed t-test for continuous variables and χ^2-test for categorical variables.

Trait	Train-val	Internal test		External test	
	Value (ref.)	Value	p-value	Value	p-value
n	50,610	8,931	–	855	–
Age at baseline (yrs)	54.89 ±7.57	54.74 ±7.68	9.80E-02	54.29 ±7.53	2.13E-02
Sex			9.18E-01		7.80E-01
Female	50.63	50.12		49.24	
Race			9.99E-01		9.64E-01
White	96.66	96.93		97.31	
Education			1.00E+00		9.99E-01
College or University degree	45.66	45.45		46.20	
Smoking			9.99E-01		4.71E-01
Never	61.57	60.83		58.83	
Alcohol			1.00E+00		9.67E-01
Three or four times a week	27.84	27.16		25.50	
BMI (Kg/m^2)	26.55 ±4.35	26.61 ±4.42	2.20E-01	26.09 ±4.38	2.51E-03
Grip strength (Kg)	30.43 ±10.61	30.68 ±10.65	4.64E-02	30.23 ±10.28	5.76E-01
HbA1c ($mmol/mol$)	35.04 ±5.09	35.07 ±5.16	7.22E-01	34.62 ±4.70	1.55E-02
HDL-C ($mmol/L$)	1.47 ±0.37	1.47 ±0.37	6.20E-01	1.46 ±0.36	3.37E-01
ApoB (g/L)	1.01 ±0.21	1.01 ±0.21	7.74E-01	1.01 ±0.22	9.84E-01
Hypertension (%)	31.03	31.51	9.18E-01	32.98	6.74E-01
Diabetes mellitus non-T1 (%)	5.56	5.78	9.26E-01	4.80	7.37E-01
Depression (%)	11.03	11.29	9.34E-01	11.93	7.73E-01

$3.06E-3$ for OnsetNet full traits) and severe vision reduction ($0.550 \pm 2.54E-3$ for OnsetNet full traits) performed best and worst on internal test respectively (Figure 3).

We analysed the importance of adding individual trait groups to model inputs (Table C10). The largest performance gains on internal test C-index from adding traits to model inputs were adding bb to demog ($\Delta 0.0542$, $p = 9.68E-15$), sbc to demog+bb ($\Delta 0.0295$, $p = 4.81E-5$), and blood to demog+bb ($\Delta 0.0272$, $p = 4.48E-4$). On internal and external test sets, utilizing body composition traits increased performance and was approximately twice as important in the absence of blood biomarkers. On internal test set C-index, adding bbc to demog+bb

Table 2: Test set performance across models measured by C-index. C-index values denote average over 47 conditions and 5 cross-valiation folds. p-values measure significance of difference with linear demog+bb+bbc+blood and were computed with two-tailed t-test. Bold font denotes top two methods for each metric.

Method	Internal test C-index	External test C-index	All test C-index
Linear			
demog+bb+bbc+blood	$6.782E-01$ $\pm 9.11E-02$	$6.435E-01$ $\pm 1.50E-01$	$6.611E-01$ $\pm 1.25E-01$
OnsetNet			
demog	$5.863E-01$ $\pm 6.96E-02$ (p=2.73E-51)	$5.683E-01$ $\pm 1.06E-01$ (p=8.05E-14)	$5.774E-01$ $\pm 9.01E-02$ (p=1.84E-45)
demog+bb	$6.404E-01$ $\pm 7.66E-02$ (p=4.55E-10)	$6.187E-01$ $\pm 1.35E-01$ (p=1.41E-02)	$6.297E-01$ $\pm 1.10E-01$ (p=1.16E-07)
demog+bb+bbc	$6.649E-01$ $\pm 7.81E-02$ (p=2.74E-02)	$6.304E-01$ $\pm 1.21E-01$ (p=1.93E-01)	$6.478E-01$ $\pm 1.03E-01$ (p=2.50E-02)
demog+bb+sbc	$6.699E-01$ $\pm 7.88E-02$ (p=1.69E-01)	$6.309E-01$ $\pm 1.23E-01$ (p=2.10E-01)	$6.506E-01$ $\pm 1.05E-01$ (p=7.68E-02)
demog+bb+blood	$6.677E-01$ $\pm 8.95E-02$ (p=8.25E-02)	$6.431E-01$ $\pm 1.34E-01$ (p=9.65E-01)	$6.555E-01$ $\pm 1.14E-01$ (p=3.48E-01)
demog+bb+bbc+blood	$6.799E-01$ $\pm 9.06E-02$ (p=7.84E-01)	$\mathbf{6.472E-01}$ $\mathbf{\pm 1.23E-01}$ **(p=7.16E-01)**	$\mathbf{6.637E-01}$ $\mathbf{\pm 1.09E-01}$ **(p=6.54E-01)**
demog+bb+sbc+blood	$\mathbf{6.820E-01}$ $\mathbf{\pm 9.02E-02}$ **(p=5.41E-01)**	$6.446E-01$ $\pm 1.27E-01$ (p=9.17E-01)	$6.635E-01$ $\pm 1.11E-01$ (p=6.85E-01)
demog+bb+bbc+sbc+blood	$\mathbf{6.830E-01}$ $\mathbf{\pm 9.02E-02}$ **(p=4.37E-01)**	$\mathbf{6.461E-01}$ $\mathbf{\pm 1.26E-01}$ **(p=7.99E-01)**	$\mathbf{6.647E-01}$ $\mathbf{\pm 1.11E-01}$ **(p=5.36E-01)**

increased performance by $\Delta 0.0244$ ($p = 6.85E-4$), sbc to demog+bb by $\Delta 0.0295$ ($p = 4.81E-5$), bbc to demog+bb+blood by $\Delta 0.0122$ ($p = 1.42E-1$), and sbc to demog+bb+blood by $\Delta 0.0143$ ($p = 8.59E-2$). For models with blood traits included, small gains were observed on internal test C-index from utilizing increasingly complex body composition inputs (demog+bb+bbc+blood: $0.6799 \pm 9.08E-2$, demog+bb+sbc+blood: $0.6820 \pm 9.04E-2$, demog+bb+bbc+sbc+blood: $0.6830 \pm$

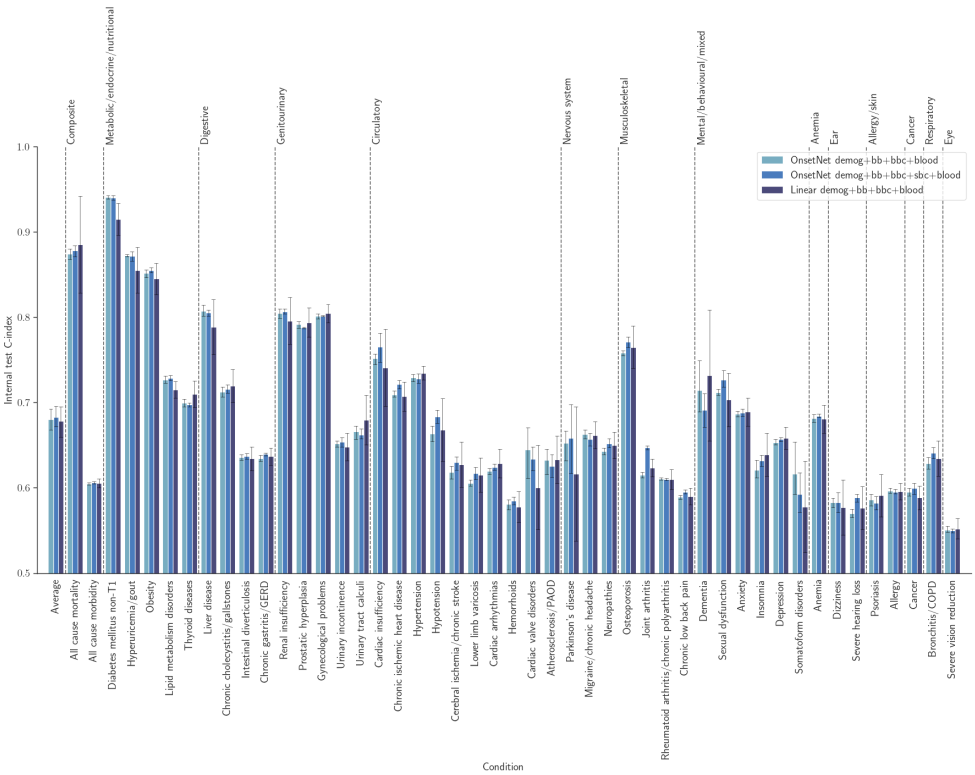

Fig. 3: Internal test set C-index across disease conditions for linear and neural network architectures. Grey error bars illustrate 95% confidence intervals.

$9.04E-2$), but performance on the external test set was highest for basic body composition (demog+bb+bbc+blood: $0.6472 \pm 1.233E-1$, demog+bb+sbc+blood: $0.6446 \pm 1.269E-1$, demog+bb+bbc+sbc+blood: $0.6461 \pm 1.264E-1$). C-index was lower ($\Delta - 0.0306 \pm 0.0080$) with higher variance on the external test set compared to the internal test set for all input trait combinations.

Following model selection and performance evaluation, the full dataset was utilized for post-hoc analysis. The best performing neural network by both average validation C-index and test C-index was demog+bb+bbc+sbc+blood which provided OnsetNet scores for analysis. Onset acceleration score quartiles were computed by discretizing

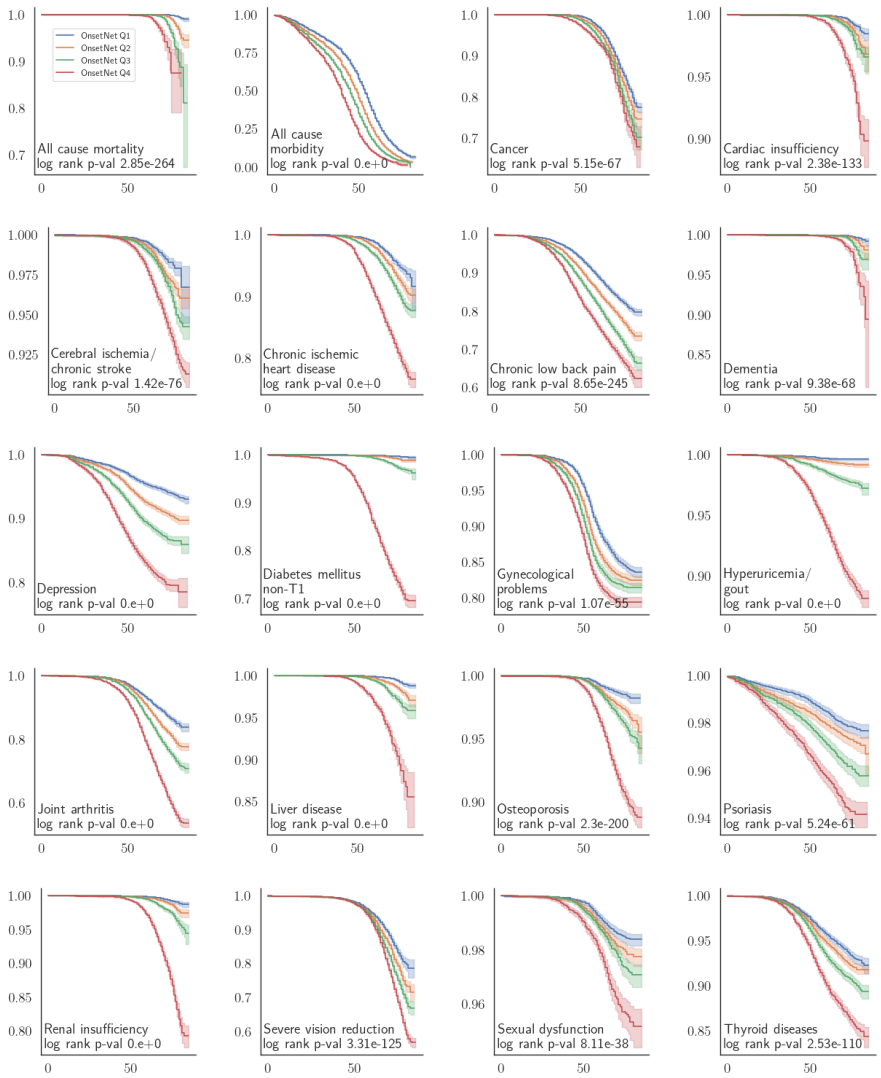

Fig. 4: Kaplan-Meier survival curves of age in years (horizontal axis) against survival probability (vertical axis) for OnsetNet risk quartiles. All conditions and at-risk counts are given in Appendix C.

OnsetNet scores using sex and condition specific quartile bins computed on the train-val dataset. Kaplan-Meier estimates for onset acceleration score quartile illustrated within-condition heterogeneity (Figure 4).

3.2 Inter-disease onset acceleration analysis

Pearson's r was computed between OnsetNet score quartiles for each pair of 38 conditions where both conditions had internal test C-index performance ≥ 0.6 (Figure 5, Figure 6). 1420 out of 1444 correlations were significant at $p \leq 3.46E-5$ level (Bonferroni corrected, $p = 5.87E-9 \pm 9.81E-8$) including all strong correlations ($r \geq 0.6$). Disease clusters and strong correlations were reproduced in sensitivity analysis without Bonferroni correction ($p \leq 0.05$) or with inclusion of statin users (Appendix C).

Onset acceleration risk quartile for all cause mortality and all cause morbidity were strongly correlated with each other ($r = 0.78$) and jointly strongly correlated with anxiety ($r = 0.86, 0.82$), dementia ($r = 0.84, 0.82$), depression ($r = 0.80, 0.83$), migraine/chronic headache ($r = 0.77, 0.69$), cardiac valve disorders ($r = 0.75, 0.65$), sexual dysfunction ($r = 0.73, 0.67$), hypotension ($r = 0.69, 0.63$), cardiac arrhythmias ($r = 0.64, 0.63$), and rheumatoid arthritis/chronic polyarthritis ($r = 0.63, 0.79$). Insomnia ($r = 0.81$), chronic gastritis/GERD ($r = 0.78$), intestinal diverticulosis ($r = 0.75$), liver disease ($r = 0.72$), cardiac insufficiency ($r = 0.69$), neuropathies ($r = 0.68$), urinary incontinence ($r = 0.68$), obesity ($r = 0.67$), and urinary tract calculi ($r = 0.63$) were strongly correlated with all cause morbidity but not with all cause mortality. Correlation between onset acceleration risk in obesity and all cause mortality was $r = 0.43$. Conversely, all cause mortality was strongly correlated with Parkinson's disease ($r = 0.72$), anemia ($r = 0.68$), and atherosclerosis/PAOD ($r = 0.62$), which were not strongly correlated with all cause morbidity. The two strongest onset acceleration correlations with Parkinson's disease were dementia ($r = 0.73$) and all cause mortality ($r = 0.72$).

Within non-composite conditions, onset acceleration risk clusters were identified by cosine distance between correlation vectors. A cardiometabolic cluster (corners of Figure 5) was identified where lipid metabolism disorders were associated with chronic ischemic heart disease ($r = 0.79$), hypertension ($r = 0.79$), cerebral ischemia/chronic

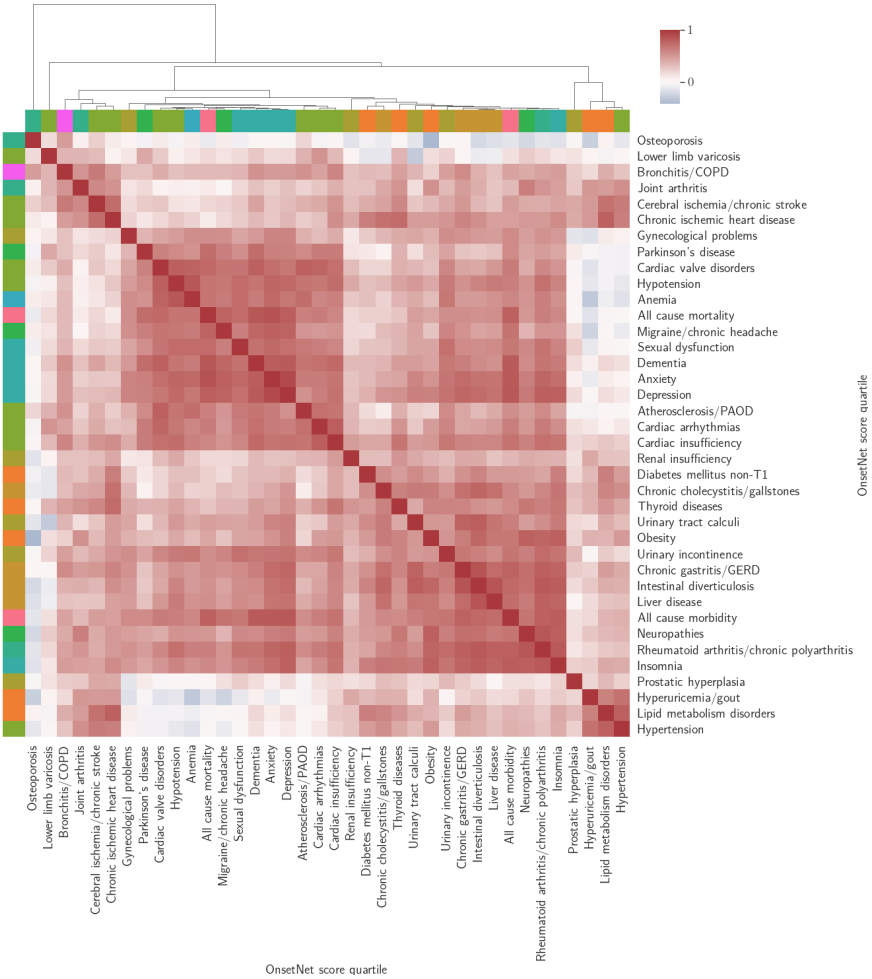

Fig. 5: Clusterplot illustrating structure in the onset acceleration risk of age-associated diseases. Onset acceleration risk quartile correlations for conditions with internal test C-index $\geq$ 0.6 were clustered by hierarchical agglomerative clustering with cosine distance between correlation vectors as the clustering metric. Color denotes risk quartile correlation strength. Statin users were removed and 24 out of 1444 entries with $p > 3.46E-5$ (Bonferroni corrected) were set to 0 for cosine distance. Row and column colours indicate condition types.

stroke ($r = 0.70$), diabetes mellitus non-T1 ($r = 0.63$), hyperuricemia/gout ($r = 0.61$), and chronic cholecystitis/gallstones ($r = 0.60$) in a cluster that did not include obesity ($r = 0.35$).

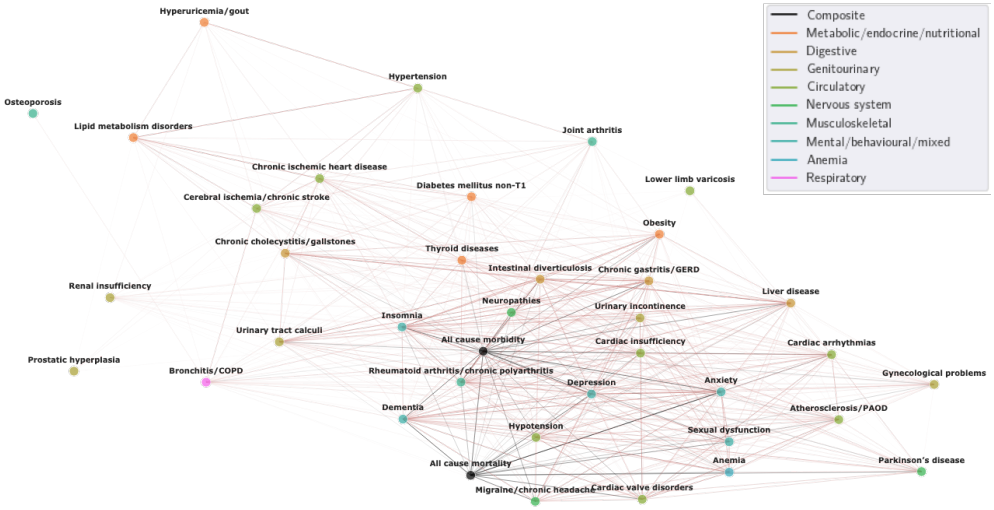

Fig. 6: Graph of inter-disease OnsetNet risk quartile correlations for conditions with internal test C-index ≥ 0.6 and correlations with $r \geq 0.3$ and $p \leq 3.46E{-}5$ (Bonferroni corrected). Statin users were removed and r scales with edge width.

Second, chronic gastritis/GERD was associated with a mixed digestive and neuropsychiatric cluster (lower right, Figure 5) containing intestinal diverticulosis ($r = 0.85$), rheumatoid arthritis/chronic polyarthritis ($r = 0.79$), all cause morbidity ($r = 0.78$), urinary tract calculi ($r = 0.77$), insomnia ($r = 0.77$), depression ($r = 0.75$), anxiety ($r = 0.73$), liver disease ($r = 0.73$), neuropathies ($r = 0.71$), chronic cholecystitis/gallstones ($r = 0.71$), urinary incontinence ($r = 0.66$), obesity ($r = 0.63$), dementia ($r = 0.63$), chronic ischemic heart disease ($r = 0.60$), cardiac insufficiency ($r = 0.60$), and thyroid diseases ($r = 0.60$).

Third, a vascular-neuropsychiatric cluster was identified (upper left, Figure 5), where onset acceleration risk in cardiac insufficiency was strongly associated with cardiac arrhythmias ($r = 0.80$), dementia ($r = 0.75$), hypotension ($r = 0.73$), rheumatoid arthritis/chronic polyarthritis ($r = 0.71$), cardiac valve disorders ($r = 0.71$), depression ($r = 0.70$), all cause morbidity ($r = 0.69$), atherosclerosis/PAOD ($r = 0.69$),

insomnia ($r = 0.68$), thyroid diseases ($r = 0.68$), anxiety ($r = 0.68$), urinary incontinence ($r = 0.67$), parkinson's disease ($r = 0.64$), anemia ($r = 0.62$), neuropathies ($r = 0.61$), chronic gastritis/GERD ($r = 0.60$), and bronchitis/COPD ($r = 0.60$).

Notable associations within the vascular-neuropsychiatric cluster included anxiety and depression ($r = 0.9$) which demonstrated the strongest correlation in onset acceleration risk overall, with top shared correlations for all cause mortality ($r = 0.86, 0.80$), all cause morbidity ($r = 0.82, 0.83$), dementia ($r = 0.81, 0.81$), migraine/chronic headache ($r = 0.78, 0.77$), rheumatoid arthritis/chronic polyarthritis ($r = 0.77, 0.79$), hypotension ($r = 0.76, 0.73$), sexual dysfunction ($r = 0.74, 0.71$), anemia ($r = 0.74, 0.67$), chronic gastritis/GERD ($r = 0.73, 0.75$), cardiac valve disorders ($r = 0.71, 0.67$), insomnia ($r = 0.71, 0.79$), intestinal diverticulosis ($r = 0.69, 0.73$), liver disease ($r = 0.69, 0.69$), cardiac insufficiency ($r = 0.68, 0.70$), urinary incontinence ($r = 0.67, 0.69$), cardiac arrhythmias ($r = 0.64, 0.63$), neuropathies ($r = 0.63, 0.66$), parkinson's disease ($r = 0.62, 0.62$), gynecological problems ($r = 0.61, 0.60$), and urinary tract calculi ($r = 0.60, 0.62$). The strongest association with anemia was hypotension and vice versa ($r = 0.84$).

3.3 Prognostic survival analysis

Adjusted hazard ratios (aHR) for OnsetNet Q4 (Q1 as reference) for 47 input conditions and 44 outcome event conditions were rendered (Figure 7). 1334 out of 2068 (64.5%) hazard ratios were significant at $p = 0.05$ level after primary adjustment without Bonferroni correction, of which Schoenfeld residuals were insignificant ($p > 0.05$) for 1238 or 92.8% ($aHR = 3.67 \pm 5.78$), and 1037 or 77.7% remained statistically significant after secondary adjustment. 435 out of 2068 (21.0%) hazard ratios were significant at $p = 9.05E-7$ level (Bonferroni corrected $p = 0.05$) after primary adjustment ($aHR = 6.11 \pm 9.00$), where all Schoenfeld residuals were insignificant ($p > 0.05$), and 184 (42.3%) remained statistically significant after secondary adjustment. With

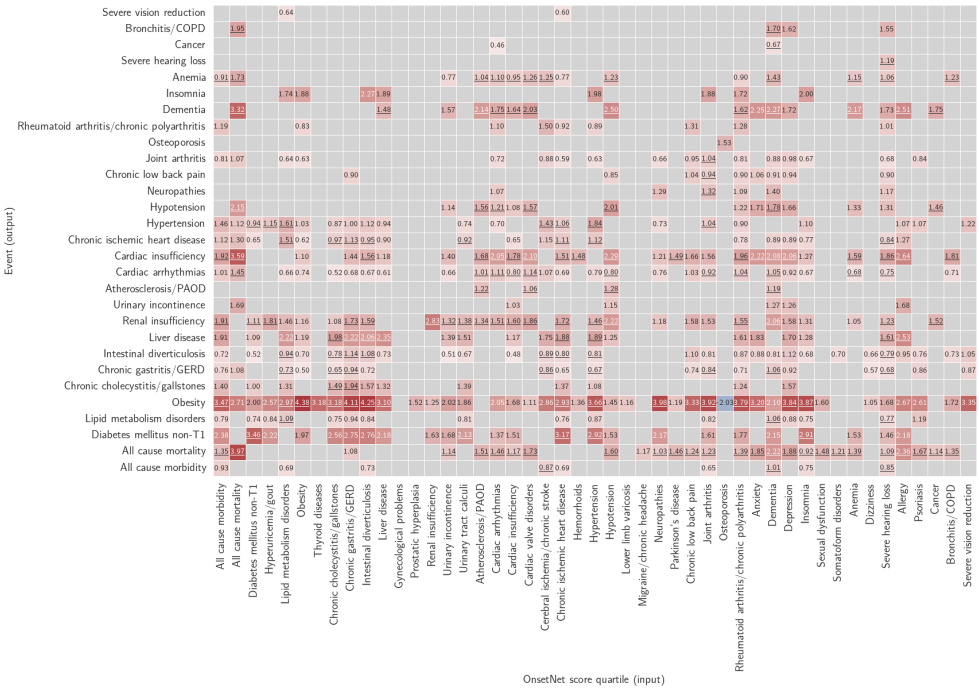

Fig. 7: Adjusted log hazard ratios for OnsetNet risk Q4 (Q1 as reference) given primary adjustment with demographic variables. Color red (blue) indicates positive (negative) log hazard ratios and color intensity scales with log hazard ratio magnitude. Gray cells denote log hazard ratios that were statistically insignificant following primary adjustment ($p > 9.05E-7$, Bonferroni corrected) or where Schoenfeld residual $p \leq 0.05$. Entries that remained statistically significant after secondary adjustment with basic body traits are underlined to denote robustness to change in adjustment.

Bonferroni correction, 25 out of 44 (56.8%) input conditions yielded statistically significant Q4 hazard ratios for the same outcome condition ($aHR = 11.09 \pm 17.8$), and 27 statistically significant Q4 hazard ratios were observed for all cause mortality ($aHR = 6.26 \pm 9.33$) of which 23 were strong with at least threefold increase in mortality risk compared to Q1 ($aHR \geq 3$, $aHR = 6.85 \pm 9.98$). Using binarized OnsetNet score instead of quartiles (above median vs. below median, Appendix C) yielded 23 statistically significant adjusted hazard ratios for all cause mortality with Bonferroni correction ($aHR = 2.24 \pm 0.408$) of which only 2 were strong (all cause mortality

and dementia, $aHR = 3.39 \pm 0.222$), suggesting that onset acceleration risk Q4 was disproportionately associated with mortality hazard compared to lower quartiles.

3.4 Biomarker saliency

To investigate the relationship learned by the neural network between input traits and onset acceleration risk of conditions, we computed sex-specific normalized absolute partial derivative of network input variables with respect to each output [44, 45]. Univariate traits (Figure 8) and multivariate spatial body composition (Figure 9) were normalized separately.

Known relationships inferred by saliency without a-priori knowledge include creatinine and cystatin C for renal insufficiency, HbA1c for diabetes mellitus non-T1, urate for hyperuricemia/gout, GGT for liver disease, total MASS for obesity, systolic blood pressure for hypertension and hypotension. Notably, BMI and total MASS were not in the top 5 traits for onset acceleration risk of diabetes mellitus non-T1, which was dominated by HbA1c. The 10 most important individual traits on average over conditions for the full traits OnsetNet model were total MASS, total SAT, total MUSC, total VAT, grip strength, GGT, HbA1c, HDL-C for both males and females, ApoB and cholesterol for males, and AST and total TMAT for females. Additional traits in the top 10 for the full univariate traits model included smoking, total TMAT, and urate for males, and alcohol, smoking and urate for females (Appendix C). The most salient spatial body composition regions were VAT and MASS located at the abdomen for males, and muscle and MASS around the abdomen for females on average over conditions. Less overt relationships inferred for both sexes included HBA1c, HDL-C and urate for anemia; GGT, ApoB, AST and body composition for dementia; urate for osteoporosis; total MASS, HBA1c and grip strength for insomnia. Total MASS was highly salient for chronic low back pain, and total TMAT was highly salient for cardiac

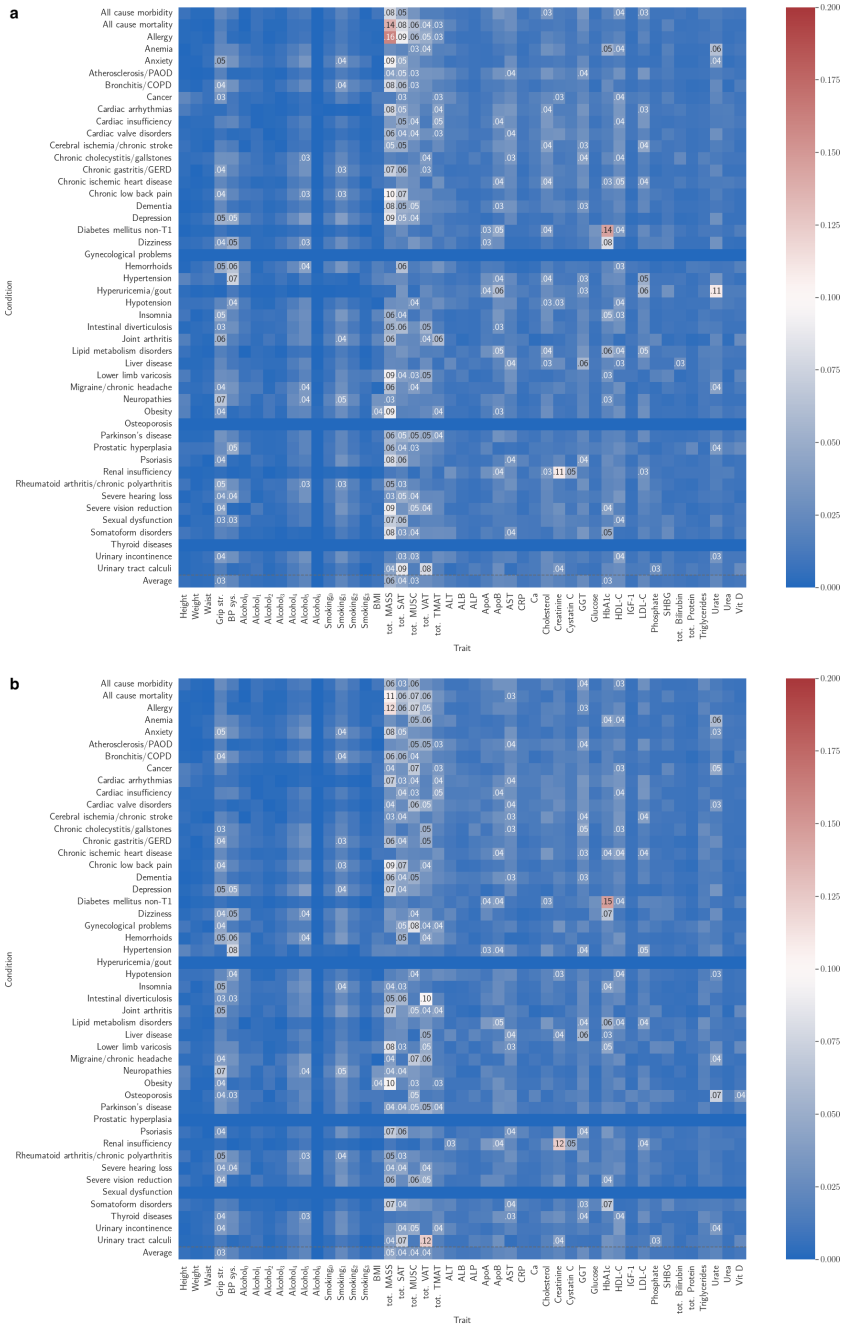

Fig. 8: Saliency map for univariate traits for (a) male and (b) female participants. Top 5 salient traits per condition are labelled. Average saliency across conditions given in the bottom row.

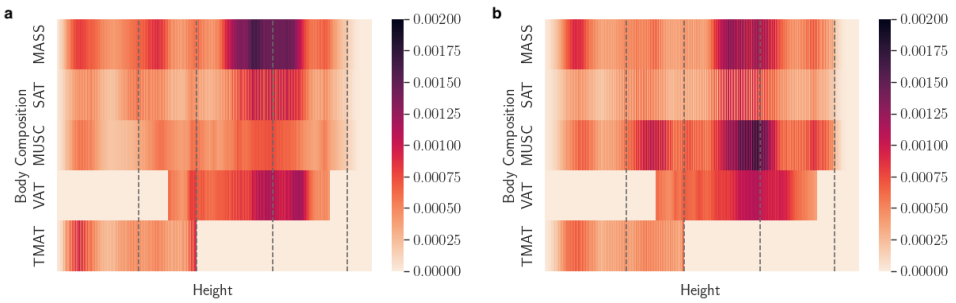

Fig. 9: Spatial body composition saliency maps averaged over 47 conditions for (a) male and (b) female participants. Condition-specific maps are given in Appendix C.5.

conditions (arrhythmias, insufficiency, valve disorders). For both sexes, body composition traits were more salient than blood biomarkers for predicting onset acceleration of dementia and Parkinson's disease; the top five univariate biomarkers for Parkinson's disease were basic body composition traits. ALT was salient for liver disease but not in the top 5 traits, which featured AST and GGT.

4 Discussion

For the methodological contribution of the study, we validated that onset acceleration risk of diverse age-associated diseases can be modelled using neural network and linear Cox architectures, with neural networks outperforming linear models on in-distribution and out-of-distribution test data. While there was high variability in predictive performance across conditions, the final model selected by cross-validation utilized all input traits and attained internal test C-index ≥ 0.6 on 38 out of 47 conditions (80.9%). Model applicability was not limited by temporal differences in trait measurement times (11.3 ± 3.03 years between blood samples and imaging scans for individuals in this study) since the relevant period is lifespan instead of post-measurement time. Inclusion of body composition was found to be important for predictive performance across disease conditions, with performance gain from adding body composition metrics to

basic demographic and anthropomorphic traits being comparable to the performance gain from adding blood biomarkers.

In post-hoc analysis, a number of connections between diseases with existing support in the literature were inferred without a-priori knowledge, such as associations in onset correlation risk between Parkinson's disease, dementia and all cause mortality, cardiovascular and cerebrovascular conditions [16, 39, 46]. Strong correlations in onset acceleration risk were inferred for cardiometabolic, digestive-neuropsychiatric, and vascular-neuropsychiatric condition groups, partially corroborating a previous review of cross-sectional multimorbidity studies across different populations which identified cardiometabolic, neuropsychiatric-gastrointestinal, and musculoskeletal-vascular-neuropsychiatric-gastrointestinal co-occurrence clusters [15] despite the use of different methodology that associated diseases by co-occurrence. Automated inference of associations between biomarkers and disease identified pre-supported associations in a precise manner, including biomarkers for renal insufficiency, diabetes and liver disease, adding to previous work that used partial derivative based saliency to identify biologically salient factors for disease [45]. Saliency analysis validated the importance of grip strength and body composition traits [47].

This study is subject to several limitations. Firstly, existing work showed that the UK Biobank cohort contains a healthy participant bias and is predominantly composed of individuals from White ethnic backgrounds [48]. Although models adjusted for sociodemographic factors, conclusions drawn may not hold for more representative or ethnically diverse populations. All conditions except all cause mortality were reliant on the timing and definition of diagnoses, which depends on factors such as access to healthcare services and diagnostic criteria. Underestimation of disease prevalence in the UK Biobank is known to occur secondary to underdiagnosis [49, 50]. While Cox models are the dominant survival analysis approach in medical research and clinical trials [51, 52] and have been used for time-to-death analysis of aging clocks [22], it is an

approximate model of survival as the proportional hazards assumption generally does not hold perfectly. In this exploratory analysis, results from evaluation against ground truth event times (Table 2, Figures 3, 4, 7) indicated that the Cox PH objective was capable of training models to predict onset acceleration risk, but alternative models may also be applied in future work. Additionally, models were assessed on held-out in-distribution and out-of-distribution test sets but are yet to be evaluated on an entirely independent cohort, and direct clinical utility and explicit causal relationships were not assessed. Prospective and intervention based studies are required to show clinical utility and support the validity of associations inferred in this study.

In summary, we introduced and evaluated the use of Cox models for modelling onset acceleration risk in the context of multimorbid aging, and performed analysis on inter-disease relationships, within-disease heterogeneity across individuals, and biomarker saliency for onset acceleration risk prediction. This work opens up novel approaches for the analysis of age-related diseases and associated biomarker predictor traits, with potential clinical applicability to early identification of high-risk groups in the population.

Declarations

Acknowledgements

The authors would like to thank the UK Biobank Reading team, Madeleine Cule, Ramprakash Srinivasan, Adam Kosiorek, and Martin Tobin for their support.

Sources of Funding

Institutional funding for the study was provided by Calico Life Sciences LLC.

Disclosures

The authors report no conflicts of interest.

Author statement

M. X. Ji conducted literature search, study design, data curation and verification, model training and data analysis, results interpretation, figures, writing first draft, and writing review and edits. M. Thanaj conducted literature search, study design, data curation and verification, results interpretation, and writing review and edits. L. Néhale-Ezzine, B. Whitcher, E. L. Thomas, and J. D. Bell conducted results interpretation, and writing review and edits.

Data access statement

Participant data from the UK Biobank cohort was obtained through UK Biobank Access Application number 44584. The UK Biobank has approval from the North West Multi-center Research Ethics Committee (REC reference: 11/NW/0382). All methods were performed in accordance with the relevant guidelines and regulations, and informed consent was obtained from all participants. Researchers may apply to use the UK Biobank data resource by submitting a health-related research proposal that is in the public interest. More information may be found on the UK Biobank researchers and resource catalogue pages (www.ukbiobank.ac.uk). No participant or public involvement occurred during the design, conduct, reporting, interpretation, or dissemination of this study.

References

[1] Barnett, K., Mercer, S.W., Norbury, M., Watt, G., Wyke, S., Guthrie, B.: Epidemiology of multimorbidity and implications for health care, research, and medical education: a cross-sectional study. The Lancet **380**(9836), 37–43 (2012)

[2] Pearson-Stuttard, J., Ezzati, M., Gregg, E.W.: Multimorbidity—a defining challenge for health systems. The Lancet Public Health **4**(12), 599–600 (2019)

[3] Valderas, J.M., Starfield, B., Sibbald, B., Salisbury, C., Roland, M.: Defining comorbidity: implications for understanding health and health services. The Annals of Family Medicine **7**(4), 357–363 (2009)

[4] Williams, J.S., Egede, L.E.: The association between multimorbidity and quality of life, health status and functional disability. The American journal of the medical sciences **352**(1), 45–52 (2016)

[5] Di Angelantonio, E., Kaptoge, S., Wormser, D., Willeit, P., Butterworth, A.S., Bansal, N., O'Keeffe, L.M., Gao, P., Wood, A.M., Burgess, S., *et al.*: Association of cardiometabolic multimorbidity with mortality. Jama **314**(1), 52–60 (2015)

[6] Frølich, A., Ghith, N., Schiøtz, M., Jacobsen, R., Stockmarr, A.: Multimorbidity, healthcare utilization and socioeconomic status: a register-based study in denmark. PloS one **14**(8), 0214183 (2019)

[7] Struijs, J.N., Baan, C.A., Schellevis, F.G., Westert, G.P., Van Den Bos, G.A.: Comorbidity in patients with diabetes mellitus: impact on medical health care utilization. BMC health services research **6**, 1–9 (2006)

[8] Uijen, A.A., Lisdonk, E.H.: Multimorbidity in primary care: prevalence and trend over the last 20 years. The European journal of general practice **14**(sup1), 28–32 (2008)

[9] Kone, A.P., Mondor, L., Maxwell, C., Kabir, U.S., Rosella, L.C., Wodchis, W.P.: Rising burden of multimorbidity and related socio-demographic factors: a repeated cross-sectional study of ontarians. Canadian Journal of Public Health **112**, 737–747 (2021)

[10] Moreno-Juste, A., Gimeno-Miguel, A., Poblador-Plou, B., Calderón-Larrañaga,

A., Del Pozo, M.C., Forjaz, M.J., Prados-Torres, A., Gimeno-Feliú, L.A.: Multimorbidity, social determinants and intersectionality in chronic patients. results from the epichron cohort. Journal of Global Health **13** (2023)

[11] Chowdhury, S.R., Das, D.C., Sunna, T.C., Beyene, J., Hossain, A.: Global and regional prevalence of multimorbidity in the adult population in community settings: a systematic review and meta-analysis. EClinicalMedicine **57** (2023)

[12] Nunes, B.P., Flores, T.R., Mielke, G.I., Thume, E., Facchini, L.A.: Multimorbidity and mortality in older adults: a systematic review and meta-analysis. Archives of gerontology and geriatrics **67**, 130–138 (2016)

[13] Tinetti, M.E., Fried, T.R., Boyd, C.M.: Designing health care for the most common chronic condition—multimorbidity. Jama **307**(23), 2493–2494 (2012)

[14] Ong, K.Y., Lee, P.S.S., Lee, E.S.: Patient-centred and not disease-focused: a review of guidelines and multimorbidity. Singapore medical journal **61**(11), 584 (2020)

[15] Prados-Torres, A., Calderón-Larrañaga, A., Hancco-Saavedra, J., Poblador-Plou, B., Akker, M.: Multimorbidity patterns: a systematic review. Journal of clinical epidemiology **67**(3), 254–266 (2014)

[16] Whitty, C.J., Watt, F.M.: Map clusters of diseases to tackle multimorbidity. Nature **579**(7800), 494–496 (2020)

[17] Ng, S.K., Tawiah, R., Sawyer, M., Scuffham, P.: Patterns of multimorbid health conditions: a systematic review of analytical methods and comparison analysis. International journal of epidemiology **47**(5), 1687–1704 (2018)

[18] Members, W.G., Lloyd-Jones, D., Adams, R., Carnethon, M., De Simone, G., Ferguson, T.B., Flegal, K., Ford, E., Furie, K., Go, A., *et al.*: Heart disease and stroke statistics—2009 update: a report from the american heart association statistics committee and stroke statistics subcommittee. Circulation **119**(3), 21–181 (2009)

[19] Lin, F.R., Thorpe, R., Gordon-Salant, S., Ferrucci, L.: Hearing loss prevalence and risk factors among older adults in the united states. Journals of Gerontology Series A: Biomedical Sciences and Medical Sciences **66**(5), 582–590 (2011)

[20] Lee, J.S., DuBois, S.G., Coccia, P.F., Bleyer, A., Olin, R.L., Goldsby, R.E.: Increased risk of second malignant neoplasms in adolescents and young adults with cancer. Cancer **122**(1), 116–123 (2016)

[21] Chao, C., Xu, L., Bhatia, S., Cooper, R., Brar, S., Wong, F.L., Armenian, S.H.: Cardiovascular disease risk profiles in survivors of adolescent and young adult (aya) cancer: the kaiser permanente aya cancer survivors study. Journal of Clinical Oncology **34**(14), 1626–1633 (2016)

[22] Lu, A.T., Quach, A., Wilson, J.G., Reiner, A.P., Aviv, A., Raj, K., Hou, L., Baccarelli, A.A., Li, Y., Stewart, J.D., *et al.*: Dna methylation grimage strongly predicts lifespan and healthspan. Aging (albany NY) **11**(2), 303 (2019)

[23] Warner, B., Ratner, E., Datta, A., Lendasse, A.: A systematic review of phenotypic and epigenetic clocks used for aging and mortality quantification in humans. Aging (Albany NY) **16**(17), 12414 (2024)

[24] Rohmann, N., Geese, T., Nestel, S., Schlicht, K., Geisler, C., Türk, K., Brix, F., Jensen-Kroll, J., Demetrowitsch, T., Bang, C., *et al.*: Metabolic and lifestyle factors accelerate disease onset and alter gut microbiome in inflammatory non-communicable diseases. BMC medicine **22**(1), 493 (2024)

[25] Sudlow, C., Gallacher, J., Allen, N., Beral, V., Burton, P., Danesh, J., Downey, P., Elliott, P., Green, J., Landray, M., *et al.*: Uk biobank: an open access resource for identifying the causes of a wide range of complex diseases of middle and old age. PLoS medicine **12**(3), 1001779 (2015)

[26] Zhang, Y., Wong, G., Mann, G., Muller, S., Yang, J.Y.: Survbenchmark: comprehensive benchmarking study of survival analysis methods using both omics data and clinical data. GigaScience **11**, 071 (2022)

[27] Wiegrebe, S., Kopper, P., Sonabend, R., Bischl, B., Bender, A.: Deep learning for survival analysis: a review. Artificial Intelligence Review **57**(3), 65 (2024)

[28] Aging Consortium, B., Herzog, C.M., Goeminne, L.J., Poganik, J.R., Barzilai, N., Belsky, D.W., Betts-LaCroix, J., Chen, B.H., Chen, M., Cohen, A.A., et al.: Challenges and recommendations for the translation of biomarkers of aging. Nature Aging, 1–12 (2024)

[29] Organization, W.H., et al.: Global status report on non-communicable diseases 2010 (2011)

[30] Torkamani, A., Andersen, K.G., Steinhubl, S.R., Topol, E.J.: High-definition medicine. Cell **170**(5), 828–843 (2017)

[31] Bera, K., Schalper, K.A., Rimm, D.L., Velcheti, V., Madabhushi, A.: Artificial intelligence in digital pathology—new tools for diagnosis and precision oncology. Nature reviews Clinical oncology **16**(11), 703–715 (2019)

[32] Collins, R.: Uk biobank: protocol for a large-scale prospective epidemiological resource (2007)

[33] Littlejohns, T.J., Holliday, J., Gibson, L.M., Garratt, S., Oesingmann, N., Alfaro-Almagro, F., Bell, J.D., Boultwood, C., Collins, R., Conroy, M.C., *et al.*: The uk biobank imaging enhancement of 100,000 participants: rationale, data collection, management and future directions. Nature communications **11**(1), 2624 (2020)

[34] Liu, Y., Basty, N., Whitcher, B., Bell, J.D., Sorokin, E.P., Bruggen, N., Thomas, E.L., Cule, M.: Genetic architecture of 11 organ traits derived from abdominal mri using deep learning. Elife **10**, 65554 (2021)

[35] Fitzpatrick, J.A., Basty, N., Cule, M., Liu, Y., Bell, J.D., Thomas, E.L., Whitcher, B.: Large-scale analysis of iliopsoas muscle volumes in the uk biobank. Scientific reports **10**(1), 20215 (2020)

[36] Thanaj, M., Basty, N., Whitcher, B., Sorokin, E.P., Liu, Y., Srinivasan, R., Cule, M., Thomas, E.L., Bell, J.D.: Precision mri phenotyping of muscle volume and quality at a population scale. Frontiers in Physiology **15**, 1288657 (2024)

[37] Whitcher, B., Thanaj, M., Cule, M., Liu, Y., Basty, N., Sorokin, E.P., Bell, J.D., Thomas, E.L.: Precision mri phenotyping enables detection of small changes in body composition for longitudinal cohorts. Scientific Reports **12**(1), 3748 (2022)

[38] Ronneberger, O., Fischer, P., Brox, T.: U-net: Convolutional networks for biomedical image segmentation. In: Medical Image Computing and Computer-assisted intervention–MICCAI 2015: 18th International Conference, Munich, Germany, October 5-9, 2015, Proceedings, Part III 18, pp. 234–241 (2015). Springer

[39] Guo, J., Huang, X., Dou, L., Yan, M., Shen, T., Tang, W., Li, J.: Aging and aging-related diseases: from molecular mechanisms to interventions and treatments. Signal Transduction and Targeted Therapy **7**(1), 391 (2022)

[40] Koller, D., Schön, G., Schäfer, I., Glaeske, G., Bussche, H., Hansen, H.: Multimorbidity and long-term care dependency—a five-year follow-up. BMC geriatrics **14**, 1–9 (2014)

[41] Katzman, J.L., Shaham, U., Cloninger, A., Bates, J., Jiang, T., Kluger, Y.: Deepsurv: personalized treatment recommender system using a cox proportional hazards deep neural network. BMC medical research methodology **18**, 1–12 (2018)

[42] Collins, G.S., Moons, K.G., Dhiman, P., Riley, R.D., Beam, A.L., Van Calster, B., Ghassemi, M., Liu, X., Reitsma, J.B., Van Smeden, M., et al.: Tripod+ ai statement: updated guidance for reporting clinical prediction models that use regression or machine learning methods. bmj **385** (2024)

[43] Von Elm, E., Altman, D.G., Egger, M., Pocock, S.J., Gøtzsche, P.C., Vandenbroucke, J.P.: The strengthening the reporting of observational studies in epidemiology (strobe) statement: guidelines for reporting observational studies. The lancet **370**(9596), 1453–1457 (2007)

[44] Selvaraju, R.R., Cogswell, M., Das, A., Vedantam, R., Parikh, D., Batra, D.: Grad-cam: Visual explanations from deep networks via gradient-based localization. In: Proceedings of the IEEE International Conference on Computer Vision, pp. 618–626 (2017)

[45] Hao, J., Kim, Y., Mallavarapu, T., Oh, J.H., Kang, M.: Interpretable deep neural network for cancer survival analysis by integrating genomic and clinical data. BMC medical genomics **12**, 1–13 (2019)

[46] Marengoni, A., Angleman, S., Melis, R., Mangialasche, F., Karp, A., Garmen, A., Meinow, B., Fratiglioni, L.: Aging with multimorbidity: a systematic review

of the literature. Ageing research reviews **10**(4), 430–439 (2011)

[47] Jung, M., Raghu, V.K., Reisert, M., Rieder, H., Rospleszcz, S., Pischon, T., Niendorf, T., Kauczor, H.-U., Völzke, H., Bülow, R., et al.: Deep learning-based body composition analysis from whole-body magnetic resonance imaging to predict all-cause mortality in a large western population. EBioMedicine **110** (2024)

[48] Fry, A., Littlejohns, T.J., Sudlow, C., Doherty, N., Adamska, L., Sprosen, T., Collins, R., Allen, N.E.: Comparison of sociodemographic and health-related characteristics of uk biobank participants with those of the general population. American journal of epidemiology **186**(9), 1026–1034 (2017)

[49] Freer, C.L., George, E.S., Tan, S.-Y., Abbott, G., Scott, D., Daly, R.M.: Prevalence of sarcopenia and its defining components in non-alcoholic fatty liver disease varies according to the method of assessment and adjustment: Findings from the uk biobank. Calcified Tissue International, 1–11 (2024)

[50] Dickey, A.K., Quick, C., Ducamp, S., Zhu, Z., Feng, Y.-C.A., Naik, H., Balwani, M., Anderson, K.E., Lin, X., Phillips, J.E., *et al.*: Evidence in the uk biobank for the underdiagnosis of erythropoietic protoporphyria. Genetics in Medicine **23**(1), 140–148 (2021)

[51] Spruance, S.L., Reid, J.E., Grace, M., Samore, M.: Hazard ratio in clinical trials. Antimicrobial agents and chemotherapy **48**(8), 2787–2792 (2004)

[52] Chen, H.-C., Kodell, R.L., Cheng, K.F., Chen, J.J.: Assessment of performance of survival prediction models for cancer prognosis. BMC medical research methodology **12**, 1–11 (2012)

Appendix A Dataset

Dataset details for $n = 60,396$ individuals are provided, including demographics, outcome counts, and biomarker descriptions.

A.1 Demographics

Table A1: Alcohol intake frequency

Sex	Alcohol intake frequency	Percentage (%)	n
Male	Daily or almost daily	22.83	6820
	Never	5.03	1503
	Once or twice a week	25.73	7685
	One to three times a month	9.11	2722
	Prefer not to answer	0.04	12
	Special occasions only	6.44	1925
	Three or four times a week	30.82	9206
	Total	100.00	29873
Female	Daily or almost daily	15.05	4595
	Never	7.22	2204
	Once or twice a week	26.71	8152
	One to three times a month	13.24	4042
	Prefer not to answer	0.02	7
	Special occasions only	13.10	3997
	Three or four times a week	24.66	7526
	Total	100.00	30523

Table A2: Smoking status

Sex	Smoking status	Percentage (%)	n
Male	Current	4.96	1481
	Never	57.70	17236
	Prefer not to answer	0.30	89
	Previous	37.05	11067
	Total	100.00	29873
Female	Current	3.62	1105
	Never	65.07	19860
	Prefer not to answer	0.33	101
	Previous	30.98	9457
	Total	100.00	30523

Table A3: Race

Sex	Race	Percentage (%)	n
Male	Asian or Asian British	1.54	461
	Black or Black British	0.53	159
	Mixed	0.32	95
	Other	0.83	247
	White	96.78	28911
	Total	100.00	29873
Female	Asian or Asian British	1.22	371
	Black or Black British	0.69	211
	Mixed	0.63	193
	Other	0.82	251
	White	96.64	29497
	Total	100.00	30523

Table A4: Education

Sex	Education	Percentage (%)	n
Male	A levels/AS levels or equivalent	11.71	3499
	College or University degree	47.23	14108
	CSEs or equivalent	4.40	1314
	None of the above	6.77	2022
	NVQ or HND or HNC or equivalent	7.98	2383
	O levels/GCSEs or equivalent	17.59	5254
	Other professional qualifications eg: nursing, teaching	3.95	1179
	Prefer not to answer	0.38	114
	Total	100.00	29873
Female	A levels/AS levels or equivalent	14.45	4412
	College or University degree	44.09	13457
	CSEs or equivalent	4.25	1296
	None of the above	6.21	1895
	NVQ or HND or HNC or equivalent	3.28	1001
	O levels/GCSEs or equivalent	21.82	6660
	Other professional qualifications eg: nursing, teaching	5.62	1716
	Prefer not to answer	0.28	86
	Total	100.00	30523

Table A5: Continuous demographic traits

	Male	**Female**
Mean birth year	1952.47	1953.92
Std birth year	7.65	7.42
Min birth year	1937.00	1937.00
Max birth year	1970.00	1970.00
IQR birth year	13.00	12.00
Mean Townsend deprivation index	-1.95	-1.86

Table A6: Assessment center

Center	**Percentage (%)**	**n**
Cheadle (imaging)	38.78	23422
Reading (imaging)	11.42	6895
Newcastle (imaging)	17.83	10766
Bristol (imaging)	1.42	855
Unknown (imaging)	30.56	18458
Total	100.00	60396

A.2 Trait distributions across dataset

Fig. A1: Demographic and basic body traits across dataset splits.

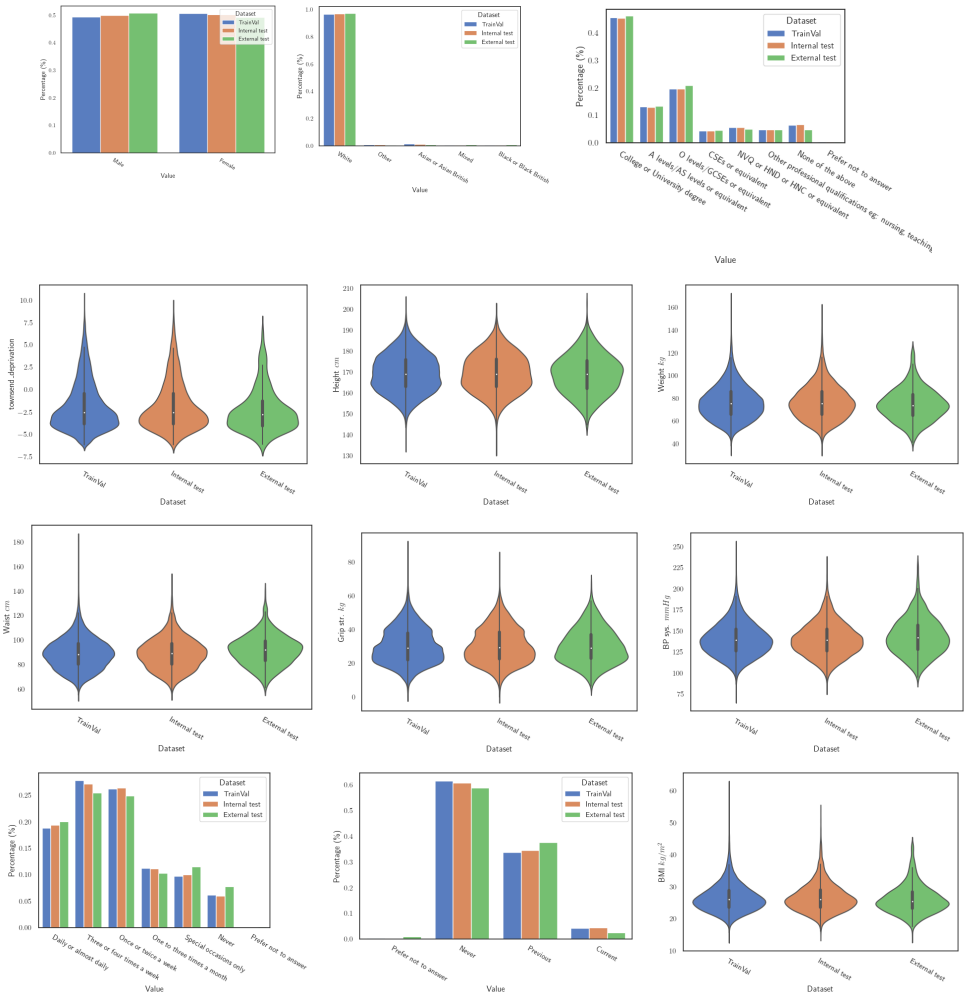

A.3 Data censoring

The UK Biobank dataset used in this study contained participants of middle age and older (50.18 years old was mean age minus two standard deviations) who had medical records collected within a finite time window, therefore data was subject to left and right censoring. Cox PH survival analysis accounted for right censoring via relative risk adjustment; participants whose medical record window were not extended late enough to include future diagnoses were optimised to have higher risk scores than people with diagnoses within the window. Limitation imposed by left censoring was ameliorated by focusing on age-associated diseases which are more prevalent from middle age onwards. Finally, large dataset size assisted the model in learning robust associations inspite of limited window size.

A.4 Disease conditions

Table A7: Non-composite condition definitions by ICD10 code.

Condition group	Condition	ICD10 codes
Metabolic/ endocrine/ nutritional	Diabetes mellitus non-T1	E11, E12, E13, E14
	Hyperuricemia/ gout	E79, M10
	Obesity	E66
	Lipid metabolism disorders	E78
	Thyroid diseases	E01, E02, E03, E04, E05, E06, E07
Genitourinary	Renal insufficiency	N18, N19
	Prostatic hyperplasia	N40
	Gynecological problems	N81, N84, N85, N86, N87, N88, N89, N90, N93, N95
	Urinary incontinence	N39, R32

Table A7 (continued)

	Urinary tract calculi	N20
Circulatory	Cardiac insufficiency	I50
	Chronic ischemic heart disease	I20, I25, I21
	Hypertension	I10, I11, I12, I13, I14, I15
	Hypotension	I95
	Cerebral ischemia/ chronic stroke	I60, I61, I62, I63, I64, I69, G45
	Lower limb varicosis	I83, I87
	Cardiac arrhythmias	I44, I45, I46, I47, I48, I49
	Hemorrhoids	I84
	Cardiac valve disorders	I34, I37
	Atherosclerosis/ PAOD	I65, I66, I67, I70, I73
Digestive	Liver disease	K70, K71, K72, K73, K74, K76
	Chronic cholecystitis/ gallstones	K80, K81
	Intestinal diverticulosis	K57
	Chronic gastritis/ GERD	K21, K25, K26, K27, K28, K29
Mental/ behavioural/ mixed	Dementia	F00, F01, F02, F03, F05, G30, G31, R54
	Sexual dysfunction	F52, N48
	Anxiety	F40, F41
	Insomnia	G47, F51
	Depression	F32, F33
	Somatoform disorders	F45
Anemia	Anemia	D50, D51, D52, D53, D55, D56, D57, D58, D59, D60, D61, D63, D64

Table A7 (continued)

Nervous system	Parkinson's disease	G20, G21, G22
	Migraine/ chronic headache	G43, G44
	Neuropathies	G50, G51, G52, G53, G54, G55, G56, G57, G58, G59, G60, G61, G62, G63, G64
Respiratory	Bronchitis/ COPD	J40, J41, J42, J43, J44, J47
Musculoskeletal	Osteoporosis	M80, M81, M82
	Joint arthritis	M15, M16, M17, M18, M19
	Rheumatoid arthritis/ chronic polyarthritis	M05, M06, M79
	Chronic low back pain	M40, M41, M42, M43, M44, M45, M47, M48, M50, M51, M52, M53, M54
Allergy/ skin	Psoriasis	L40
	Allergy	H01, J30, L23, L27, L56, K52, K90, T78, T88
Eye	Severe vision reduction	H17, H18, H25, H26, H27, H28, H31, H33, H34, H35, H36, H40, H43, H47, H54
Ear	Dizziness	H81, H82, R42
	Severe hearing loss	H90, H91

Table A7 (continued)

Cancer	Cancer	C00, C01, C02, C03, C04, C05, C06, C07, C08, C09, C10, C11, C12, C13, C14, C15, C16, C17, C18, C19, C20, C21, C22, C23, C24, C25, C26, C30, C31, C32, C33, C34, C35, C36, C37, C38, C39, C40, C41, C43, C44, C45, C46, C47, C48, C49, C50, C51, C52, C53, C54, C55, C56, C57, C58, C60, C61, C62, C63, C64, C65, C66, C67, C68, C69, C70, C71, C72, C73, C74, C75, C76, C77, C78, C79, C80, C81, C82, C83,C84, C85, C86, C87, C88, C89, C90, C91, C92, C93, C94, C95, C96, C97, D00, D01, D02, D03, D04, D05, D06, D07, D08, D09, D37, D38, D39, D40, D41, D42, D43, D44, D45, D46, D47, D48

Table A8: Condition event counts.

Condition	**Male**	**Female**
All cause morbidity	26335	27318
All cause mortality	277	146
Allergy	5835	6380
Anemia	1559	3020
Anxiety	1571	2728
Atherosclerosis/PAOD	796	807
Bronchitis/COPD	1571	1441

Table A8 (continued)

Cancer	3865	3570
Cardiac arrhythmias	3122	1758
Cardiac insufficiency	508	185
Cardiac valve disorders	317	219
Cerebral ischemia/chronic stroke	1130	676
Chronic cholecystitis/gallstones	1185	2177
Chronic gastritis/GERD	6472	6220
Chronic ischemic heart disease	3220	1253
Chronic low back pain	6352	6903
Dementia	169	107
Depression	2497	4194
Diabetes mellitus non-T1	2215	1158
Dizziness	475	791
Gynecological problems	4	10193
Hemorrhoids	1925	1672
Hypertension	11184	7618
Hyperuricemia/gout	1725	173
Hypotension	554	467
Insomnia	1135	775
Intestinal diverticulosis	3676	3367
Joint arthritis	5267	6513
Lipid metabolism disorders	8400	4681
Liver disease	642	556
Lower limb varicosis	1124	1756
Migraine/chronic headache	1422	3249
Neuropathies	2217	2954
Obesity	1956	1823
Osteoporosis	318	1825

Table A8 (continued)

Parkinson's disease	96	46
Prostatic hyperplasia	4425	2
Psoriasis	1015	908
Renal insufficiency	997	815
Rheumatoid arthritis/chronic polyarthritis	4145	5153
Severe hearing loss	1294	865
Severe vision reduction	5048	5203
Sexual dysfunction	1063	105
Somatoform disorders	123	207
Thyroid diseases	1058	3907
Urinary incontinence	1529	3475
Urinary tract calculi	1016	418

A.5 Quartile definitions

Table A9: OnsetNet score quartile boundaries computed for the best model (demog+bb+bbc+sbc+blood) from the train-val dataset.

Condition	**Male**			**Female**		
	Q1 end	Q2 end	Q3 end	Q1 end	Q2 end	Q3 end
All cause morbidity	0.403	0.629	0.869	0.531	0.761	1.016
All cause mortality	-0.289	1.610	3.678	-0.772	0.963	2.914
Allergy	0.471	0.693	0.943	0.502	0.678	0.888
Anemia	-1.593	-1.263	-0.895	-1.077	-0.527	0.102
Anxiety	-0.037	0.415	0.905	0.582	1.009	1.523
Atherosclerosis/PAOD	0.139	0.511	0.903	0.121	0.533	0.958
Bronchitis/COPD	0.390	0.750	1.136	0.402	0.721	1.048
Cancer	-0.881	-0.788	-0.684	-1.011	-0.762	-0.373

Table A9 (continued)

Cardiac arrhythmias	-0.156	0.134	0.442	-0.674	-0.390	-0.065
Cardiac insufficiency	0.337	0.918	1.529	-0.601	-0.043	0.580
Cardiac valve disorders	-1.962	-1.542	-1.102	-2.396	-1.856	-1.254
Cerebral ischemia/chronic stroke	1.351	1.683	2.056	0.788	1.079	1.420
Chronic cholecystitis/gallstones	-1.013	-0.588	-0.183	-0.539	-0.069	0.505
Chronic gastritis/GERD	0.110	0.414	0.734	-0.009	0.291	0.630
Chronic ischemic heart disease	0.446	0.885	1.399	-0.674	-0.242	0.281
Chronic low back pain	-0.204	0.018	0.244	-0.122	0.100	0.332
Dementia	-1.546	-0.749	0.086	-1.812	-1.049	-0.223
Depression	-1.068	-0.657	-0.220	-0.473	-0.098	0.321
Diabetes mellitus non-T1	-1.534	-0.389	1.001	-2.371	-1.346	-0.071
Dizziness	-1.028	-0.817	-0.611	-0.438	-0.198	0.047
Gynecological problems	-2.602	-2.414	-2.192	2.871	3.068	3.244
Hemorrhoids	-0.109	0.071	0.287	-0.405	-0.199	0.049
Hypertension	2.360	2.897	3.462	1.762	2.289	2.892
Hyperuricemia/gout	1.538	2.436	3.370	-1.022	-0.314	0.569
Hypotension	-2.655	-2.119	-1.492	-3.003	-2.327	-1.525
Insomnia	0.593	1.034	1.574	0.349	0.654	1.042
Intestinal diverticulosis	-0.645	-0.328	0.035	-0.769	-0.478	-0.138
Joint arthritis	-0.260	0.026	0.338	-0.043	0.272	0.622
Lipid metabolism disorders	1.175	1.696	2.277	0.407	0.931	1.495
Liver disease	-2.166	-1.368	-0.404	-2.284	-1.524	-0.610
Lower limb varicosis	-0.014	0.257	0.519	0.562	0.820	1.080
Migraine/chronic headache	-0.332	-0.071	0.201	0.468	0.774	1.075
Neuropathies	0.229	0.518	0.848	0.485	0.773	1.102

Table A9 (continued)

Obesity	-0.204	0.776	1.834	-0.821	0.193	1.460
Osteoporosis	-1.091	-0.697	-0.260	0.695	1.149	1.619
Parkinson's disease	1.555	2.370	3.106	0.437	1.174	1.921
Prostatic hyperplasia	3.460	3.740	4.024	-1.954	-1.698	-1.408
Psoriasis	1.084	1.387	1.668	0.769	1.079	1.401
Renal insufficiency	-2.061	-1.331	-0.523	-1.946	-1.279	-0.528
Rheumatoid arthritis/chronic polyarthritis	-0.549	-0.311	-0.061	-0.359	-0.098	0.196
Severe hearing loss	-0.498	-0.349	-0.192	-0.934	-0.781	-0.610
Severe vision reduction	1.281	1.457	1.609	1.390	1.551	1.715
Sexual dysfunction	1.134	1.380	1.652	-1.461	-1.139	-0.658
Somatoform disorders	0.152	0.518	0.839	0.486	0.931	1.340
Thyroid diseases	-0.640	-0.421	-0.162	0.708	0.931	1.191
Urinary incontinence	-0.404	-0.240	-0.054	0.419	0.677	0.980
Urinary tract calculi	-0.231	0.077	0.410	-1.140	-0.861	-0.542

A.6 Data pre-processing

The UK Biobank study protocol is publically available [25]. The inclusion flowchart is given in A2.

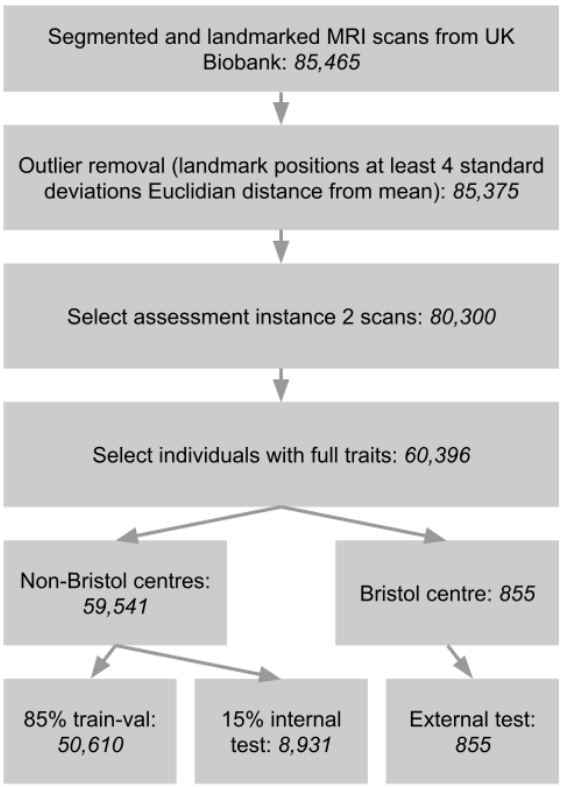

Fig. A2: Pre-processing flowchart for data utilized in the study.

Body composition variables

The sbc variable with dimension $[5 \times 370]$ consisted of mass, subcutaneous adipose tissue, muscle, visceral adipose tissue, thigh intramuscular and intermuscular adipose tissue channels measured along 370 vertical slices, segmented and landmarked (at mid-thigh, hip, T12 vertebra as top of the iliopsoas muscle, and shoulder) with a previously published deep learning system [34–37]. Spatial body composition was computed from tissue segmentation maps by summing tissue volume for each vertical slice to yield a $[1 \times 370]$ vector per tissue type along the height dimension, followed by linear interpolation to register vectors to sex-specific average landmark positions and concatenation to combine vectors into a matrix with dimension $[5 \times 370]$.

Appendix B Architecture

OnsetNet's architecture is illustrated in Figure B3.

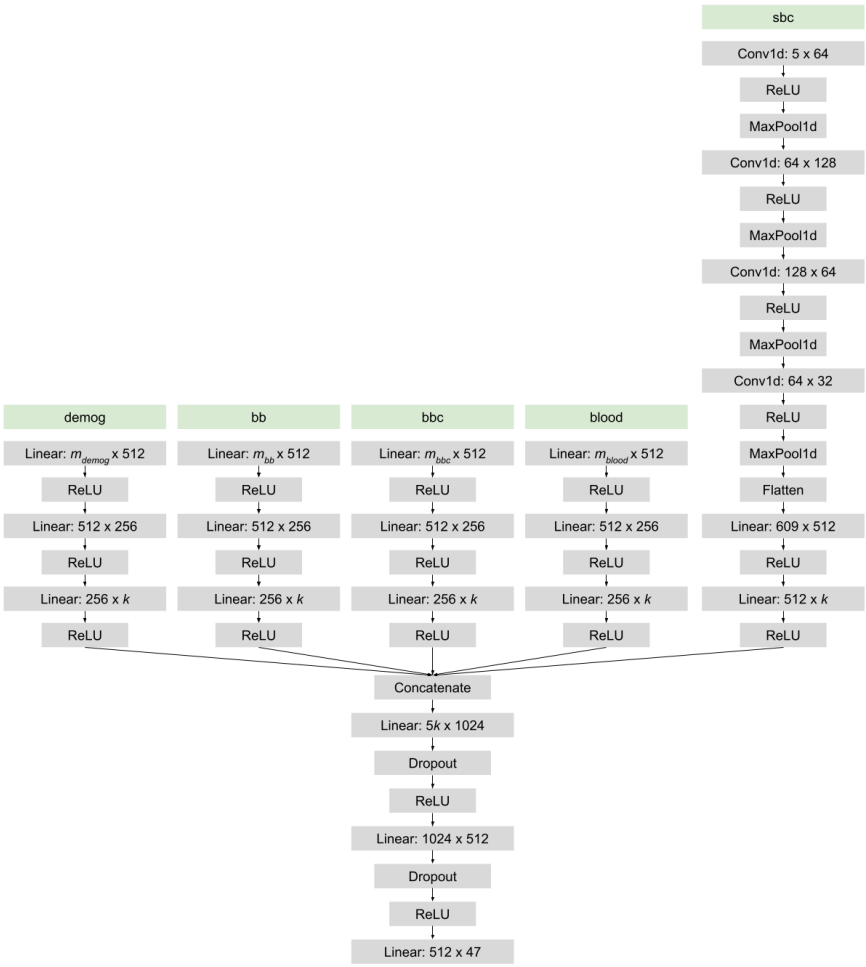

Fig. B3: Architecture for neural network OnsetNet with channel sizes and PyTorch naming convention. Input variables shown in green. m_g denotes input dimensions of trait group g. Encoders produce feature vectors of fixed length $k \in \{128, 256, 512\}$, where k is a hyperparameter.

Appendix C Additional Results

C.1 Addition of biomarker inputs

Table C10: Difference in internal test C-index from adding additional input types to change from input type 1 to input type 2. C-index values denote average over 47 conditions and 5 folds. * (**) denotes significance at $p = 0.05$ (Bonferroni corrected $p = 2.27E - 3$) level.

Input type 1		Input type 2		Difference	P-value
Name	C-index	Name	C-index		
demog	5.863E-1	demog+bb	6.404E-1	5.415E-2	9.676E-15 **
demog	5.863E-1	demog+bb+bbc	6.649E-1	7.859E-2	4.274E-27 **
demog	5.863E-1	demog+bb+sbc	6.699E-1	8.362E-2	8.809E-30 **
demog	5.863E-1	demog+bb+blood	6.677E-1	8.137E-2	4.182E-25 **
demog	5.863E-1	demog+bb+bbc blood	6.799E-1	9.362E-2	2.851E-31 **
demog	5.863E-1	demog+bb+sbc blood	6.82E-1	9.567E-2	1.523E-32 **
demog	5.863E-1	demog+bb+bbc sbc+blood	6.83E-1	9.668E-2	3.973E-33 **
demog+bb	6.404E-1	demog+bb+bbc	6.649E-1	2.444E-2	6.848E-4 **
demog+bb	6.404E-1	demog+bb+sbc	6.699E-1	2.947E-2	4.805E-5 **
demog+bb	6.404E-1	demog+bb+blood	6.677E-1	2.722E-2	4.478E-4 **
demog+bb	6.404E-1	demog+bb+bbc blood	6.799E-1	3.947E-2	5.225E-7 **
demog+bb	6.404E-1	demog+bb+sbc blood	6.82E-1	4.152E-2	1.265E-7 **
demog+bb	6.404E-1	demog+bb+bbc sbc+blood	6.83E-1	4.253E-2	6.294E-8 **

Table C10 (continued)

demog+bb+bbc	6.649E-1	demog+bb+bbc blood	6.799E-1	1.503E-2	5.523E-2
demog+bb+bbc	6.649E-1	demog+bb+bbc sbc+blood	6.83E-1	1.809E-2	2.078E-2 *
demog+bb+sbc	6.699E-1	demog+bb+sbc blood	6.82E-1	1.205E-2	1.246E-1
demog+bb+sbc	6.699E-1	demog+bb+bbc sbc+blood	6.83E-1	1.306E-2	9.595E-2
demog+bb+blood	6.677E-1	demog+bb+bbc blood	6.799E-1	1.224E-2	1.42E-1
demog+bb+blood	6.677E-1	demog+bb+sbc blood	6.82E-1	1.43E-2	8.59E-2
demog+bb+blood	6.677E-1	demog+bb+bbc sbc+blood	6.83E-1	1.531E-2	6.594E-2
demog+bb+bbc blood	6.799E-1	demog+bb+bbc sbc+blood	6.83E-1	3.062E-3	7.142E-1
demog+bb+sbc blood	6.82E-1	demog+bb+bbc sbc+blood	6.83E-1	1.01E-3	9.037E-1

C.2 Test performance

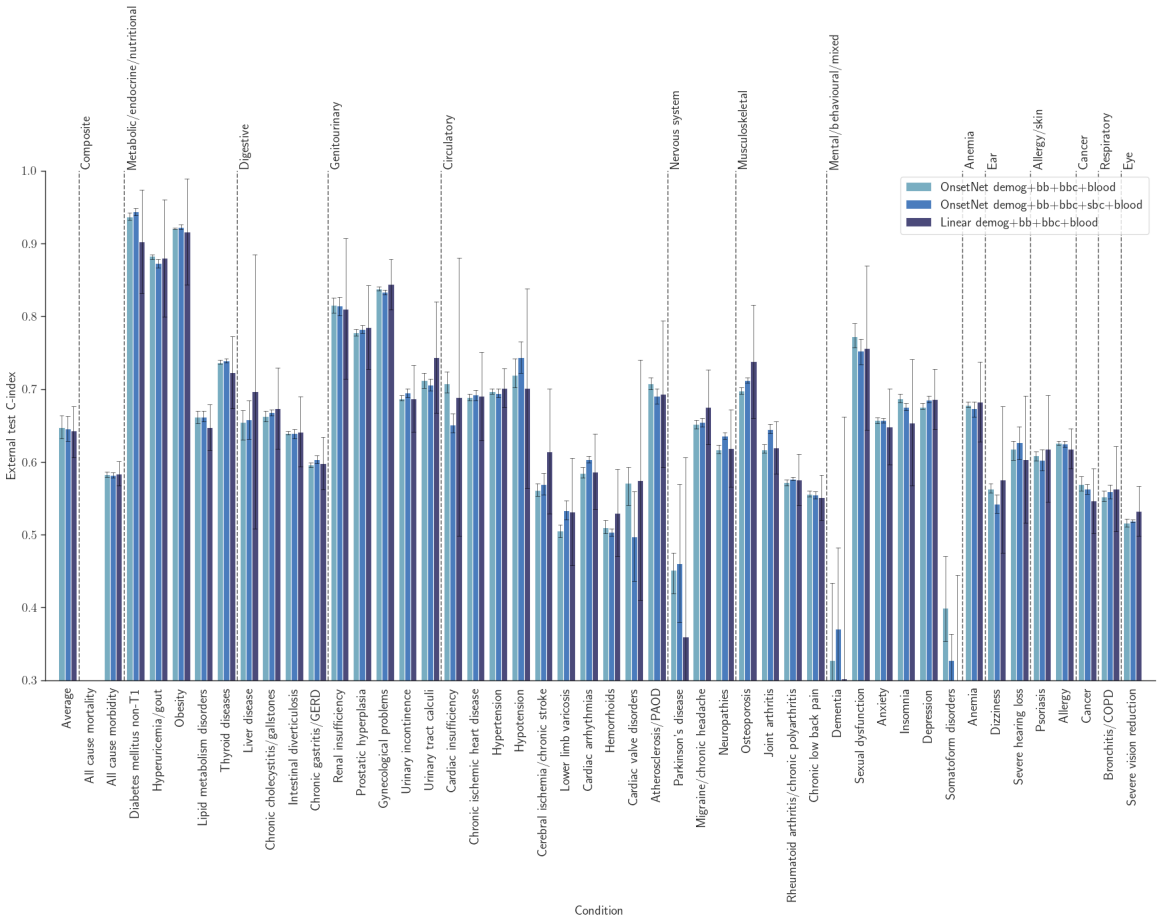

Fig. C4: External test set C-index across disease conditions for neural network and linear architectures. Gray error bars illustrate 95% confidence intervals.

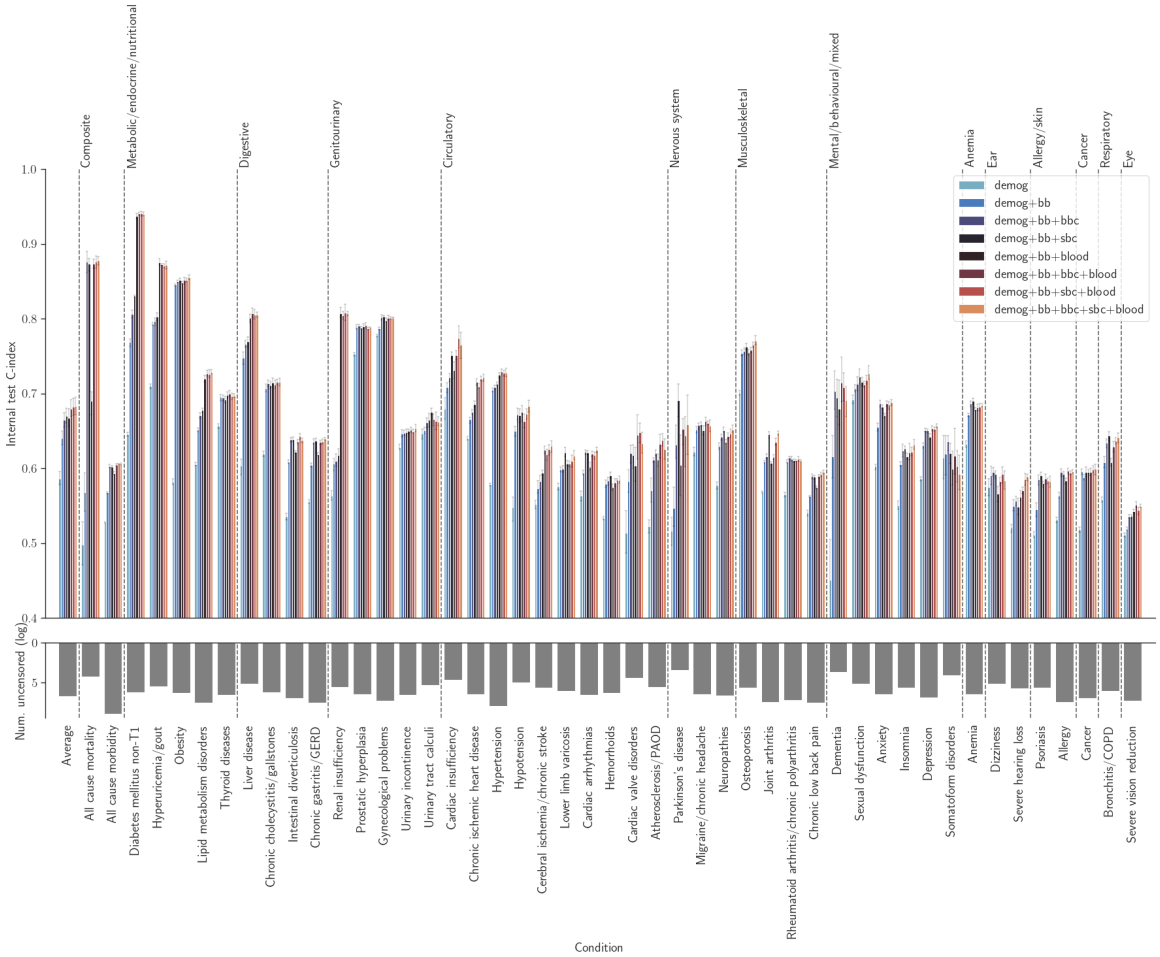

Fig. C5: Internal test set C-index across disease conditions for neural network architectures. Gray error bars illustrate 95% confidence intervals.

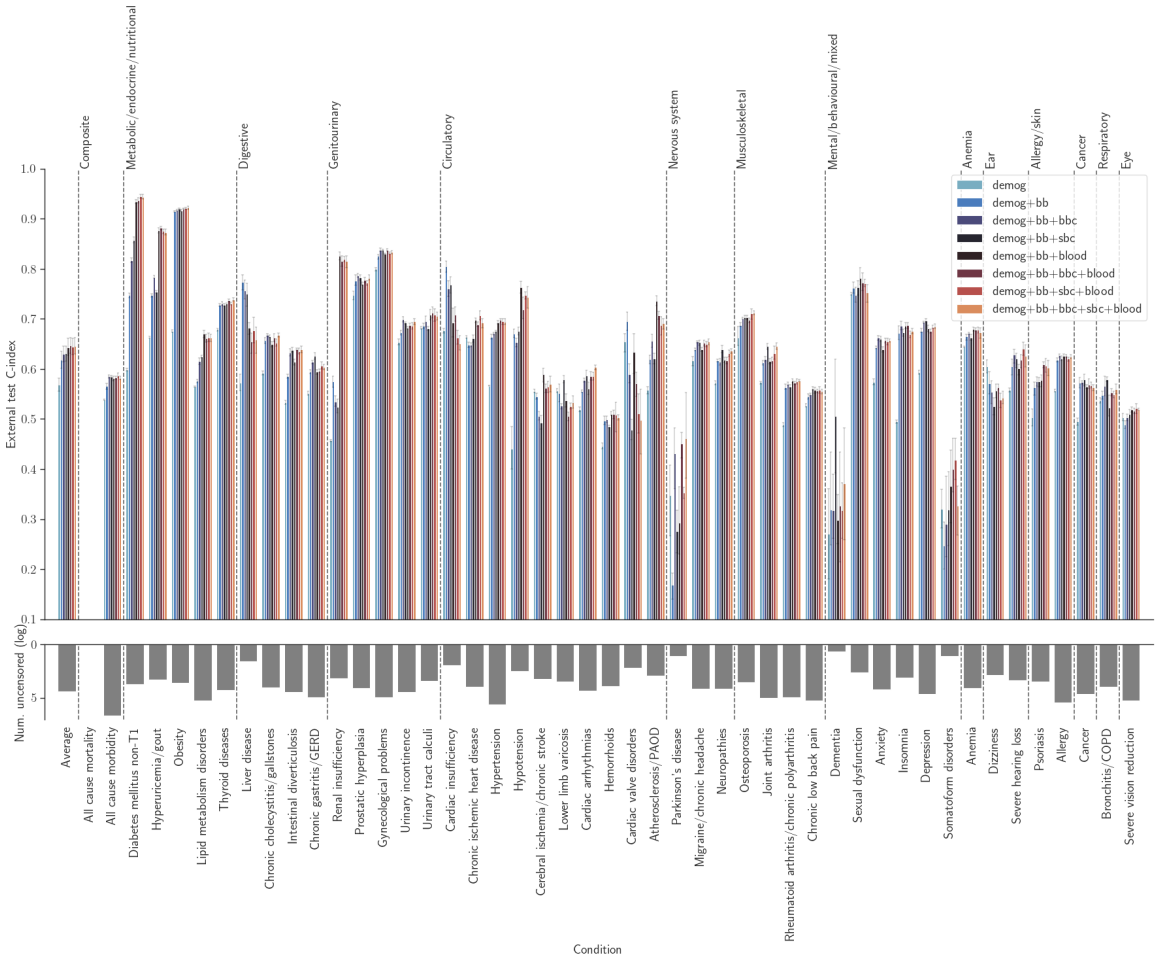

Fig. C6: External test set C-index across disease conditions for neural network architectures. Gray error bars illustrate 95% confidence intervals.

C.3 Kaplan-Meier curves

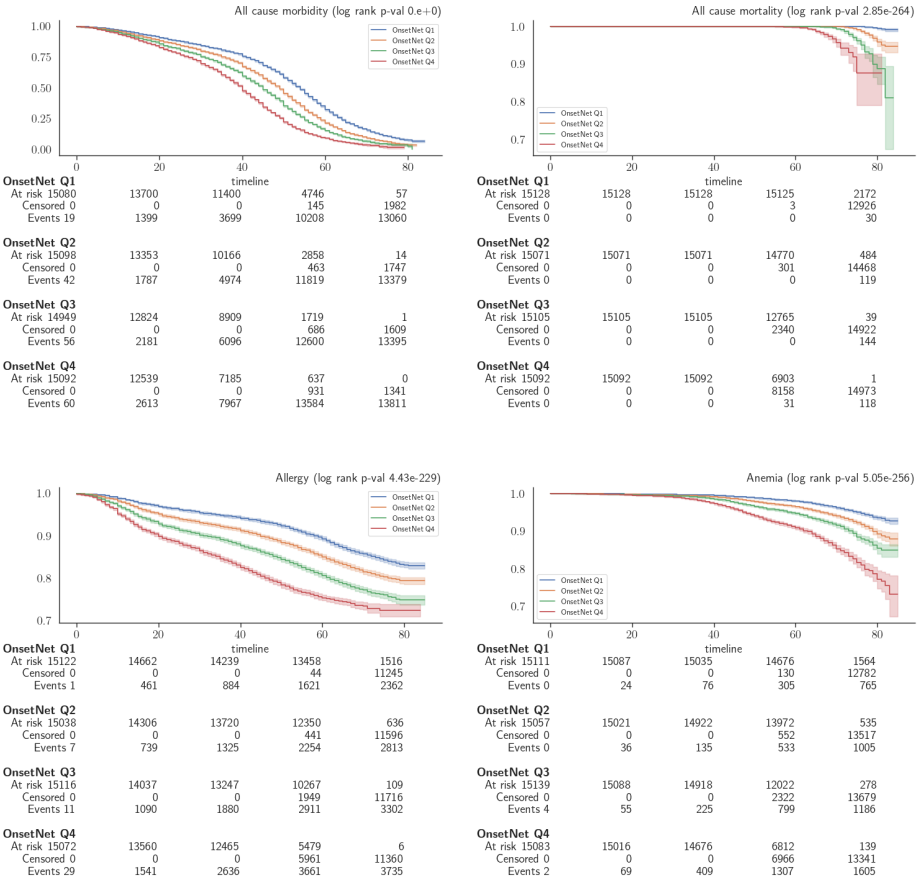

Fig. C7: Kaplan-Meier curves plotting survival probability (vertical) against age in years (horizontal). (1/9)

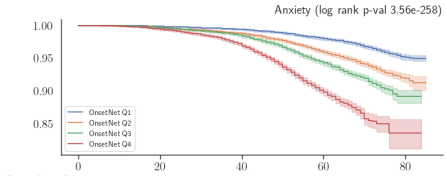

OnsetNet Q1				
At risk 15055	15031	14965	14728	2013
Censored 0	0	0	25	12424
Events 0	24	90	302	618
OnsetNet Q2				
At risk 15108	15057	14918	14007	500
Censored 0	0	0	492	13662
Events 1	52	191	610	947
OnsetNet Q3				
At risk 15079	15019	14830	11940	96
Censored 0	0	0	2287	13858
Events 1	61	250	853	1126
OnsetNet Q4				
At risk 15152	15062	14683	6590	12
Censored 0	0	0	7102	13538
Events 0	90	469	1460	1602

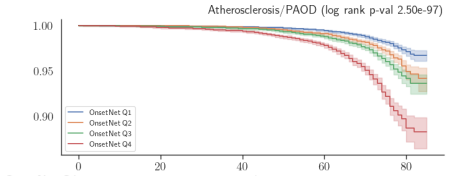

OnsetNet Q1				
At risk 15038	15030	15016	14485	1148
Censored 0	0	0	467	13629
Events 1	9	23	87	262
OnsetNet Q2				
At risk 15151	15148	15121	13445	683
Censored 0	0	0	1567	14122
Events 0	3	30	139	346
OnsetNet Q3				
At risk 15119	15104	15068	11965	478
Censored 0	0	0	2972	14257
Events 2	17	53	184	386
OnsetNet Q4				
At risk 15084	15048	14986	9131	306
Censored 0	0	0	5639	14181
Events 1	37	99	315	598

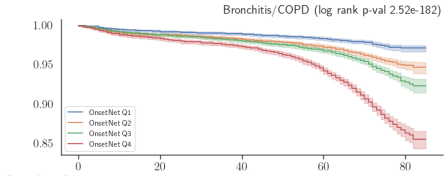

OnsetNet Q1				
At risk 15091	14978	14929	12259	435
Censored 0	0	0	2584	14332
Events 7	120	169	255	331
OnsetNet Q2				
At risk 15131	14957	14867	12136	619
Censored 0	0	0	2589	13953
Events 8	182	272	414	567
OnsetNet Q3				
At risk 15109	14929	14812	12001	750
Censored 0	0	0	2630	13643
Events 7	187	304	485	723
OnsetNet Q4				
At risk 15033	14782	14634	11469	727
Censored 0	0	0	2722	12934
Events 10	261	409	852	1382

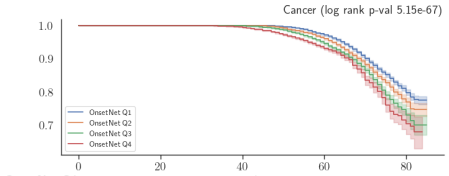

OnsetNet Q1				
At risk 15171	15171	15171	14715	1491
Censored 0	0	0	17	11379
Events 0	0	0	439	2301
OnsetNet Q2				
At risk 15023	15023	15023	14271	389
Censored 0	0	0	153	12548
Events 0	0	0	599	2086
OnsetNet Q3				
At risk 15121	15121	15105	13198	205
Censored 0	0	0	1114	13147
Events 0	0	16	809	1769
OnsetNet Q4				
At risk 15081	15081	14990	5224	77
Censored 0	0	0	8937	13780
Events 0	0	91	920	1224

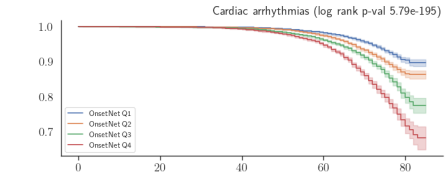

OnsetNet Q1				
At risk 15112	15105	15075	14389	987
Censored 0	0	0	442	13209
Events 1	8	38	282	917
OnsetNet Q2				
At risk 15077	15068	15023	13274	627
Censored 0	0	0	1410	13344
Events 1	10	55	394	1107
OnsetNet Q3				
At risk 15110	15092	15014	11564	429
Censored 0	0	0	2987	13394
Events 2	20	98	561	1289
OnsetNet Q4				
At risk 15093	15073	14973	8727	248
Censored 0	0	0	5622	13305
Events 0	20	120	744	1540

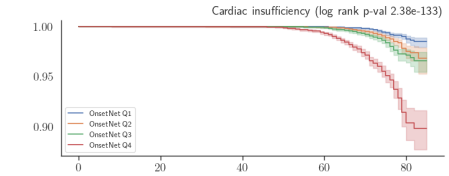

OnsetNet Q1				
At risk 15082	15082	15081	14468	1269
Censored 0	0	0	608	13729
Events 0	0	1	6	84
OnsetNet Q2				
At risk 15202	15202	15200	13191	648
Censored 0	0	0	1998	14442
Events 0	0	2	13	112
OnsetNet Q3				
At risk 14960	14960	14960	11592	471
Censored 0	0	0	3348	14358
Events 0	0	0	20	131
OnsetNet Q4				
At risk 15152	15151	15150	10212	272
Censored 0	0	0	4844	14522
Events 0	1	2	96	358

Fig. C8: Kaplan-Meier curves plotting survival probability (vertical) against age in years (horizontal). (2/9)

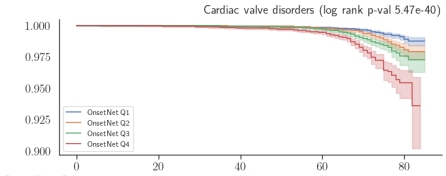

OnsetNet Q1				
At risk	15170	15169	15162	14965	1488
Censored	0	0	0	181	13583
Events	1	2	9	25	100
OnsetNet Q2				
At risk	15057	15056	15051	14176	693
Censored	0	0	0	850	14239
Events	0	1	6	31	125
OnsetNet Q3				
At risk	15090	15089	15081	12480	347
Censored	0	0	0	2567	14607
Events	0	1	9	43	136
OnsetNet Q4				
At risk	15078	15075	15050	7819	169
Censored	0	0	0	7180	14740
Events	0	3	28	79	169

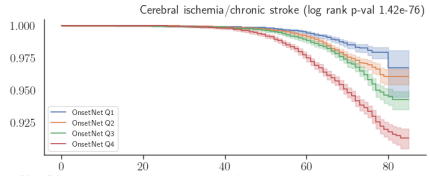

OnsetNet Q1				
At risk	15135	15132	15119	11431	70
Censored	0	0	0	3621	14897
Events	0	3	16	83	168
OnsetNet Q2				
At risk	15104	15101	15086	12182	275
Censored	0	0	0	2798	14511
Events	0	3	18	124	318
OnsetNet Q3				
At risk	15092	15092	15070	12496	744
Censored	0	0	0	2427	13893
Events	2	2	24	171	457
OnsetNet Q4				
At risk	15062	15061	15033	12807	1454
Censored	0	0	0	1888	12753
Events	1	2	30	368	856

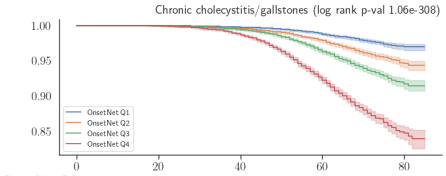

OnsetNet Q1				
At risk	15090	15088	15053	12961	649
Censored	0	0	0	1950	14127
Events	0	2	37	179	314
OnsetNet Q2				
At risk	15127	15121	15064	12316	756
Censored	0	0	0	2492	13814
Events	0	6	63	319	557
OnsetNet Q3				
At risk	15099	15094	15007	11965	756
Censored	0	0	0	2586	13467
Events	0	5	92	548	876
OnsetNet Q4				
At risk	15080	15073	14878	10572	379
Censored	0	0	0	3381	13093
Events	0	7	202	1127	1608

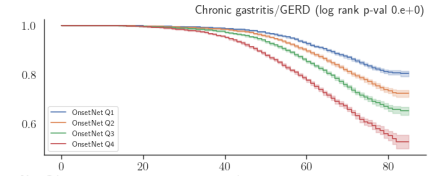

OnsetNet Q1				
At risk	15113	15083	14923	13284	763
Censored	0	0	0	716	12182
Events	0	30	190	1113	2168
OnsetNet Q2				
At risk	15081	15041	14830	11987	643
Censored	0	0	0	1551	11602
Events	3	43	254	1546	2839
OnsetNet Q3				
At risk	15055	14992	14641	10487	419
Censored	0	0	0	2423	11162
Events	0	63	414	2145	3474
OnsetNet Q4				
At risk	15144	15066	14409	7418	146
Censored	0	0	0	4501	10807
Events	0	78	735	3225	4191

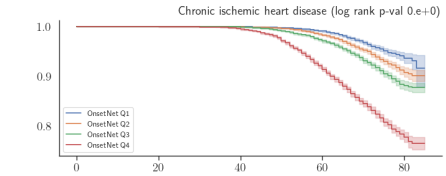

OnsetNet Q1				
At risk	15142	15141	15137	11620	272
Censored	0	0	0	3385	14466
Events	0	1	5	137	404
OnsetNet Q2				
At risk	15054	15053	15042	12071	537
Censored	0	0	0	2737	13823
Events	0	1	12	246	694
OnsetNet Q3				
At risk	15154	15152	15135	12314	725
Censored	0	0	0	2412	13387
Events	0	2	19	428	1042
OnsetNet Q4				
At risk	15046	15039	14959	11727	758
Censored	0	0	0	2068	11974
Events	0	7	87	1251	2314

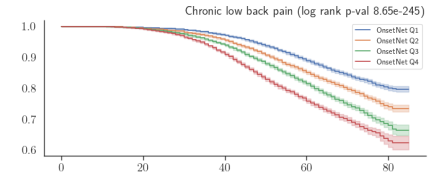

OnsetNet Q1				
At risk	15140	15088	14712	12934	1017
Censored	0	0	0	547	11580
Events	2	54	430	1661	2545
OnsetNet Q2				
At risk	15135	15052	14459	11538	587
Censored	0	0	0	1363	11460
Events	2	85	678	2236	3090
OnsetNet Q3				
At risk	15017	14916	14102	9835	360
Censored	0	0	0	2446	11065
Events	5	106	920	2741	3597
OnsetNet Q4				
At risk	15094	14962	13731	7103	107
Censored	0	0	0	4474	10981
Events	1	133	1364	3518	4007

Fig. C9: Kaplan-Meier curves plotting survival probability (vertical) against age in years (horizontal). (3/9)

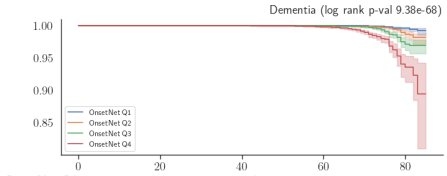

OnsetNet Q1				
At risk	15213	15213	14844	1462
Censored	0	0	0	365	13718
Events	0	0	0	4	33
OnsetNet Q2				
At risk	15101	15100	15099	13557	739
Censored	0	0	0	1536	14315
Events	0	1	2	8	47
OnsetNet Q3				
At risk	15045	15044	15044	12139	378
Censored	0	0	0	2899	14595
Events	0	1	1	7	72
OnsetNet Q4				
At risk	15037	15036	15034	8996	128
Censored	0	0	0	6009	14794
Events	0	1	3	32	115

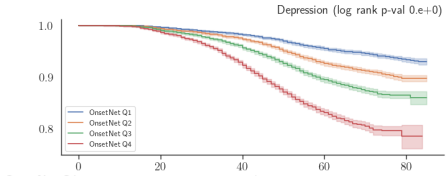

OnsetNet Q1				
At risk	15129	15075	14860	14311	1824
Censored	0	0	0	133	12391
Events	0	54	269	685	914
OnsetNet Q2				
At risk	15078	14987	14680	13003	555
Censored	0	0	0	965	13178
Events	0	91	398	1110	1345
OnsetNet Q3				
At risk	15080	14939	14415	10840	152
Censored	0	0	0	2668	13143
Events	0	141	665	1572	1785
OnsetNet Q4				
At risk	15109	14905	13933	6971	28
Censored	0	0	0	5649	12439
Events	0	204	1176	2489	2642

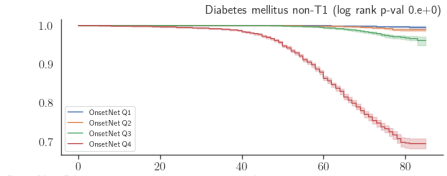

OnsetNet Q1				
At risk	15091	15091	15091	13463	627
Censored	0	0	0	1615	14430
Events	0	0	0	13	34
OnsetNet Q2				
At risk	15064	15063	15061	12628	742
Censored	0	0	0	2407	14240
Events	1	2	4	30	83
OnsetNet Q3				
At risk	15214	15213	15210	11925	678
Censored	0	0	0	3203	14292
Events	0	1	4	86	244
OnsetNet Q4				
At risk	15026	14973	14785	9798	438
Censored	0	0	0	3292	11580
Events	0	53	241	1936	3008

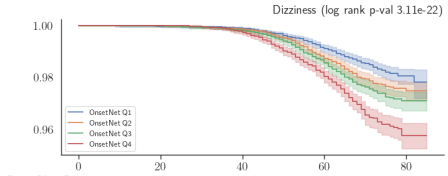

OnsetNet Q1				
At risk	15112	15108	15093	13508	678
Censored	0	0	0	1472	14212
Events	0	4	19	132	222
OnsetNet Q2				
At risk	15118	15116	15097	12785	645
Censored	0	0	0	2146	14183
Events	0	2	21	187	290
OnsetNet Q3				
At risk	15049	15047	15018	12051	624
Censored	0	0	0	2787	14099
Events	0	2	31	211	326
OnsetNet Q4				
At risk	15117	15117	15078	10543	735
Censored	0	0	0	4292	13955
Events	0	0	39	282	427

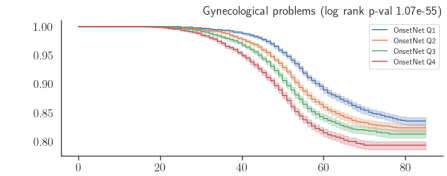

OnsetNet Q1				
At risk	14979	14976	14796	12832	1136
Censored	0	0	0	509	11599
Events	0	3	183	1638	2244
OnsetNet Q2				
At risk	15103	15099	14753	11751	624
Censored	0	0	0	1251	12005
Events	0	4	350	2101	2474
OnsetNet Q3				
At risk	15120	15110	14633	10308	425
Censored	0	0	0	2436	12082
Events	0	10	487	2376	2613
OnsetNet Q4				
At risk	15193	15168	14424	7651	228
Censored	0	0	0	4817	12101
Events	1	26	770	2726	2865

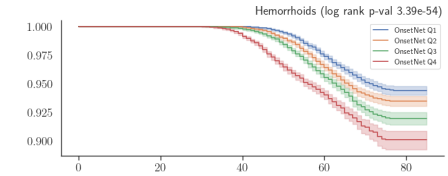

OnsetNet Q1				
At risk	15108	15108	15106	14670	960
Censored	0	0	0	42	13376
Events	0	0	2	396	772
OnsetNet Q2				
At risk	15091	15091	15078	14157	864
Censored	0	0	0	395	13346
Events	0	0	13	539	881
OnsetNet Q3				
At risk	15046	15046	15012	12070	540
Censored	0	0	0	2319	13554
Events	0	0	34	657	952
OnsetNet Q4				
At risk	15151	15151	15015	6702	173
Censored	0	0	0	7599	13986
Events	0	0	136	850	992

Fig. C10: Kaplan-Meier curves plotting survival probability (vertical) against age in years (horizontal). (4/9)

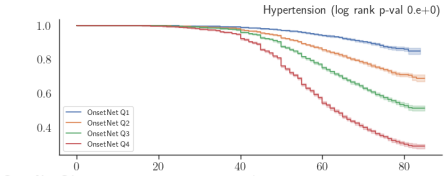

OnsetNet Q1				
At risk 15136	15119	14958	10020	172
Censored 0	0	0	4281	13757
Events 1	18	179	836	1208
OnsetNet Q2				
At risk 15049	15028	14644	10509	403
Censored 0	0	0	2438	11536
Events 1	22	406	2103	3111
OnsetNet Q3				
At risk 15129	15102	14525	9931	435
Censored 0	0	0	1499	9200
Events 0	27	604	3699	5494
OnsetNet Q4				
At risk 15080	15017	13890	7390	306
Censored 0	0	0	934	5812
Events 0	63	1190	6756	8962

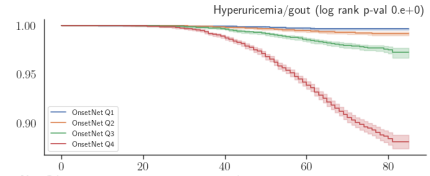

OnsetNet Q1				
At risk 15233	15230	15221	10723	150
Censored 0	0	0	4466	15035
Events 0	3	12	44	48
OnsetNet Q2				
At risk 15087	15085	15059	12063	470
Censored 0	0	0	2942	14514
Events 0	2	28	82	103
OnsetNet Q3				
At risk 15012	15009	14956	12757	789
Censored 0	0	0	2040	13923
Events 0	3	56	215	300
OnsetNet Q4				
At risk 15064	15058	14870	12955	1208
Censored 0	0	0	1203	12415
Events 0	6	194	906	1441

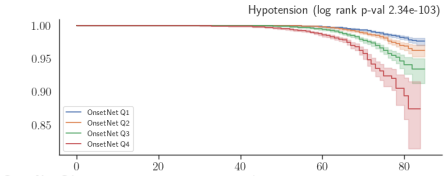

OnsetNet Q1				
At risk 15207	15207	15206	15168	1790
Censored 0	0	0	11	13217
Events 0	0	1	28	200
OnsetNet Q2				
At risk 15009	15009	15008	14769	611
Censored 0	0	0	205	14171
Events 0	0	1	35	227
OnsetNet Q3				
At risk 15065	15065	15064	12979	230
Censored 0	0	0	1997	14551
Events 0	0	1	89	284
OnsetNet Q4				
At risk 15115	15114	15094	6425	44
Censored 0	0	0	8505	14773
Events 0	1	21	185	298

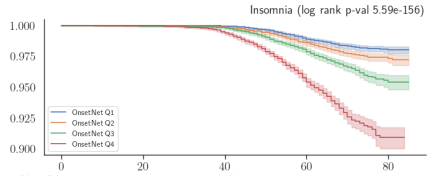

OnsetNet Q1				
At risk 15144	15143	15133	14501	1285
Censored 0	0	0	474	13596
Events 0	1	11	169	263
OnsetNet Q2				
At risk 15040	15039	15017	13188	743
Censored 0	0	0	1638	13973
Events 0	1	23	214	324
OnsetNet Q3				
At risk 15044	15039	15011	11502	448
Censored 0	0	0	3236	14135
Events 1	6	34	307	462
OnsetNet Q4				
At risk 15167	15165	15075	9307	177
Censored 0	0	0	5209	14130
Events 0	2	92	651	860

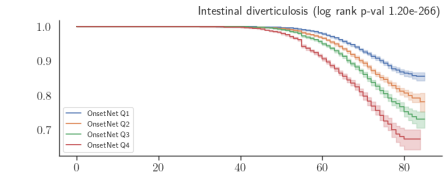

OnsetNet Q1				
At risk 15123	15120	15108	14653	993
Censored 0	0	0	151	12740
Events 0	3	15	319	1390
OnsetNet Q2				
At risk 15090	15086	15068	13527	794
Censored 0	0	0	1058	12497
Events 0	4	22	505	1799
OnsetNet Q3				
At risk 15053	15052	15038	11577	376
Censored 0	0	0	2757	12774
Events 0	1	15	719	1903
OnsetNet Q4				
At risk 15130	15126	15085	7674	64
Censored 0	0	0	6201	13141
Events 0	4	45	1255	1925

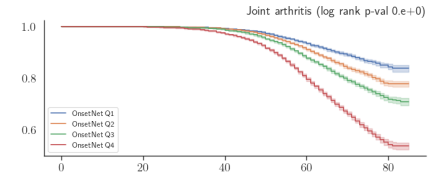

OnsetNet Q1				
At risk 15212	15204	15089	10526	409
Censored 0	0	0	3722	13324
Events 0	8	123	964	1479
OnsetNet Q2				
At risk 15096	15093	14955	11205	497
Censored 0	0	0	2588	12378
Events 0	3	141	1303	2221
OnsetNet Q3				
At risk 15098	15084	14890	11187	550
Censored 0	0	0	2114	11545
Events 0	14	208	1797	3003
OnsetNet Q4				
At risk 14990	14966	14561	10517	480
Censored 0	0	0	1472	9446
Events 0	24	429	3001	5064

Fig. C11: Kaplan-Meier curves plotting survival probability (vertical) against age in years (horizontal). (5/9)

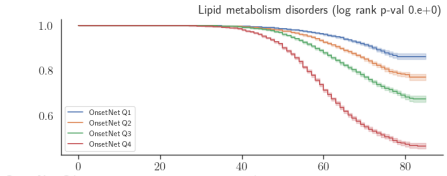

OnsetNet Q1				
At risk	15108	15106	15045	9762	101
Censored	0	0	0	4783	14047
Events	0	2	63	563	960
OnsetNet Q2				
At risk	15064	15062	14971	11514	384
Censored	0	0	0	2491	12603
Events	0	2	93	1059	2077
OnsetNet Q3				
At risk	15163	15160	15030	11704	603
Censored	0	0	0	1671	11137
Events	0	3	133	1788	3423
OnsetNet Q4				
At risk	15058	15054	14749	9777	555
Censored	0	0	0	1045	7904
Events	3	7	312	4239	6602

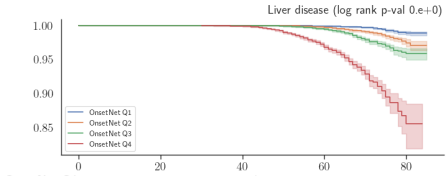

OnsetNet Q1				
At risk	15111	15110	15110	15017	1695
Censored	0	0	0	82	13318
Events	0	1	1	12	98
OnsetNet Q2				
At risk	15026	15026	15026	14194	727
Censored	0	0	0	794	14118
Events	0	0	0	38	181
OnsetNet Q3				
At risk	15107	15107	15105	11838	235
Censored	0	0	0	3193	14616
Events	0	0	2	76	256
OnsetNet Q4				
At risk	15151	15151	15134	8150	37
Censored	0	0	0	6578	14456
Events	1	1	18	424	659

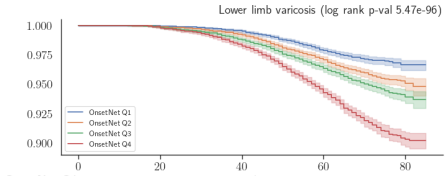

OnsetNet Q1				
At risk	14999	14992	14927	11553	468
Censored	0	0	0	3137	14141
Events	2	9	74	311	392
OnsetNet Q2				
At risk	15188	15172	15065	11872	591
Censored	0	0	0	2883	14017
Events	1	17	124	434	581
OnsetNet Q3				
At risk	15139	15110	14950	12091	676
Censored	0	0	0	2506	13742
Events	0	29	189	542	721
OnsetNet Q4				
At risk	15067	15037	14802	12281	858
Censored	0	0	0	1939	13026
Events	0	30	265	847	1183

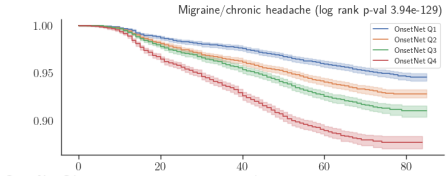

OnsetNet Q1				
At risk	15055	14857	14687	14198	1554
Censored	0	0	0	253	12750
Events	0	198	368	604	751
OnsetNet Q2				
At risk	15109	14822	14527	13104	685
Censored	0	0	0	1117	13412
Events	1	288	583	889	1013
OnsetNet Q3				
At risk	15087	14757	14388	11473	304
Censored	0	0	0	2509	13574
Events	2	332	701	1107	1211
OnsetNet Q4				
At risk	15139	14604	14027	7521	65
Censored	0	0	0	5981	13382
Events	3	538	1115	1640	1695

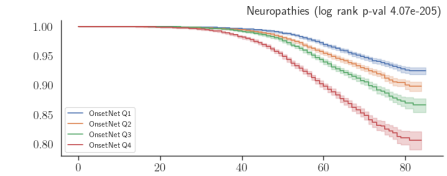

OnsetNet Q1				
At risk	15144	15140	15086	14097	1227
Censored	0	0	0	584	13039
Events	2	6	60	465	880
OnsetNet Q2				
At risk	15073	15061	14983	12636	677
Censored	0	0	0	1765	13312
Events	1	13	91	673	1085
OnsetNet Q3				
At risk	15028	15022	14902	11220	419
Censored	0	0	0	2933	13293
Events	1	7	127	876	1317
OnsetNet Q4				
At risk	15147	15127	14866	8904	171
Censored	0	0	0	4777	13093
Events	0	20	281	1466	1883

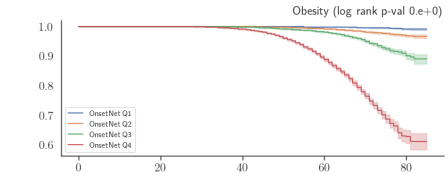

OnsetNet Q1				
At risk	15141	15141	15138	14521	1366
Censored	0	0	0	592	13696
Events	0	0	3	28	79
OnsetNet Q2				
At risk	15072	15071	15061	12753	690
Censored	0	0	0	2202	14108
Events	0	1	11	117	274
OnsetNet Q3				
At risk	15090	15089	15063	11561	423
Censored	0	0	0	3241	13963
Events	0	1	27	288	704
OnsetNet Q4				
At risk	15093	15089	14954	9278	119
Censored	0	0	0	4243	12260
Events	0	4	139	1572	2714

Fig. C12: Kaplan-Meier curves plotting survival probability (vertical) against age in years (horizontal). (6/9)

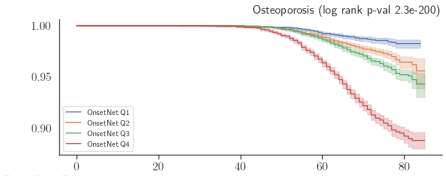

OnsetNet Q1				
At risk	15054	15044	10513	246
Censored	0	0	4434	14651
Events	0	10	107	157
OnsetNet Q2				
At risk	15141	15133	12078	550
Censored	0	0	2896	14278
Events	1	8	167	313
OnsetNet Q3				
At risk	15176	15170	12836	772
Censored	0	0	2137	13948
Events	0	6	203	456
OnsetNet Q4				
At risk	15024	15003	13222	1001
Censored	0	0	1263	12817
Events	1	2	22	540
1207				

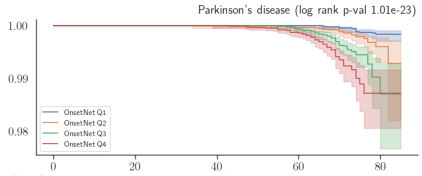

OnsetNet Q1				
At risk	15120	15120	14493	1937
Censored	0	0	627	13167
Events	0	0	0	16
OnsetNet Q2				
At risk	15069	15068	13117	548
Censored	0	0	1947	14498
Events	0	1	5	23
OnsetNet Q3				
At risk	15136	15136	11952	195
Censored	0	0	3174	14895
Events	0	0	10	46
OnsetNet Q4				
At risk	15071	15070	9984	61
Censored	0	0	5067	14954
Events	0	1	20	56

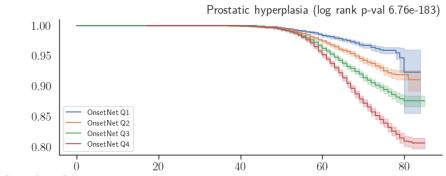

OnsetNet Q1				
At risk	15064	15060	11170	21
Censored	0	0	3664	14670
Events	0	4	230	373
OnsetNet Q2				
At risk	15093	15081	12018	116
Censored	0	0	2700	14226
Events	0	12	375	751
OnsetNet Q3				
At risk	15205	15197	12406	448
Censored	0	0	2251	13519
Events	0	8	548	1238
OnsetNet Q4				
At risk	15033	15032	15022	12262	1615
Censored	0	0	2078	11361
Events	1	2	12	694	2058

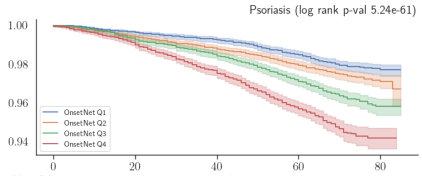

OnsetNet Q1				
At risk	15035	14980	14922	14088	926
Censored	0	0	0	721	13802
Events	2	57	115	228	309
OnsetNet Q2				
At risk	15178	15090	14991	13318	908
Censored	0	0	0	1550	13891
Events	2	90	189	312	381
OnsetNet Q3				
At risk	15029	14920	14796	12042	590
Censored	0	0	0	2561	13920
Events	3	112	236	429	522
OnsetNet Q4				
At risk	15141	14996	14772	8853	233
Censored	0	0	0	5655	14204
Events	6	151	375	639	710

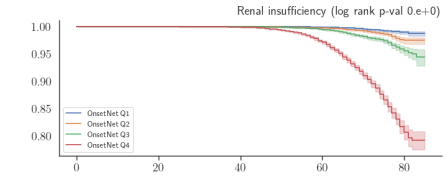

OnsetNet Q1				
At risk	15219	15218	15218	13923	747
Censored	0	0	0	1276	14388
Events	0	1	1	20	84
OnsetNet Q2				
At risk	15058	15056	15051	12273	634
Censored	0	0	0	2743	14283
Events	0	2	7	42	141
OnsetNet Q3				
At risk	15061	15061	15059	11539	596
Censored	0	0	0	3446	14200
Events	0	0	2	76	265
OnsetNet Q4				
At risk	15058	15054	15034	11398	556
Censored	0	0	0	3257	13194
Events	0	4	24	403	1308

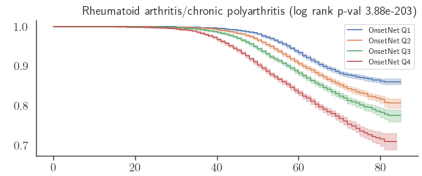

OnsetNet Q1				
At risk	15209	15200	15139	14079	1201
Censored	0	0	0	115	12135
Events	0	9	70	1015	1873
OnsetNet Q2				
At risk	15048	15036	14927	12673	587
Censored	0	0	0	959	12264
Events	0	12	121	1416	2197
OnsetNet Q3				
At risk	14997	14986	14771	10423	371
Censored	0	0	0	2847	12266
Events	0	11	226	1727	2360
OnsetNet Q4				
At risk	15142	15121	14635	7222	120
Censored	0	0	0	5507	12166
Events	0	21	507	2413	2856

Fig. C13: Kaplan-Meier curves plotting survival probability (vertical) against age in years (horizontal). (7/9)

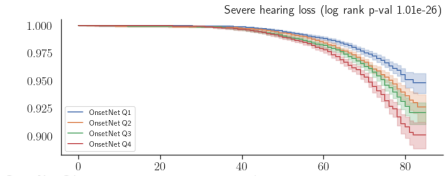

OnsetNet Q1				
At risk 15202	15200	15180	14039	584
Censored 0	0	0	984	14213
Events 0	2	22	179	405
OnsetNet Q2				
At risk 15089	15077	15049	12756	732
Censored 0	0	0	2102	13828
Events 0	12	40	231	529
OnsetNet Q3				
At risk 15039	15029	14986	11736	648
Censored 0	0	0	3035	13826
Events 0	10	53	268	565
OnsetNet Q4				
At risk 15066	15060	15011	10230	589
Censored 0	0	0	4522	13831
Events 0	6	55	314	646

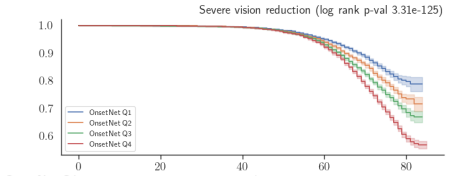

OnsetNet Q1				
At risk 14984	14973	14905	10508	83
Censored 0	0	0	3755	13524
Events 5	16	84	726	1382
OnsetNet Q2				
At risk 15210	15199	15107	11210	211
Censored 0	0	0	3117	13034
Events 3	14	106	886	1968
OnsetNet Q3				
At risk 15129	15110	15026	12121	298
Censored 0	0	0	1978	12119
Events 7	26	110	1037	2719
OnsetNet Q4				
At risk 15055	15037	14948	12435	1059
Censored 0	0	0	1469	9857
Events 3	21	110	1154	4142

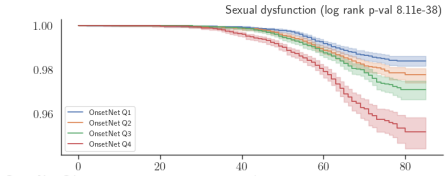

OnsetNet Q1				
At risk 15168	15167	15156	14964	891
Censored 0	0	0	78	14058
Events 0	1	12	126	219
OnsetNet Q2				
At risk 15074	15073	15052	14428	770
Censored 0	0	0	477	14030
Events 0	1	22	169	274
OnsetNet Q3				
At risk 15040	15039	15021	12713	622
Censored 0	0	0	2144	14124
Events 0	1	19	183	294
OnsetNet Q4				
At risk 15114	15110	15052	6855	405
Censored 0	0	0	7973	14328
Events 0	4	62	286	381

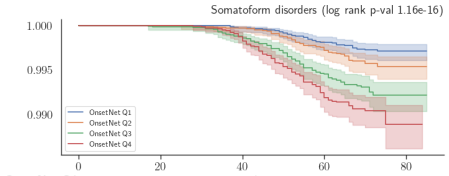

OnsetNet Q1				
At risk 15071	15071	15067	14044	1304
Censored 0	0	0	999	13727
Events 0	0	4	28	40
OnsetNet Q2				
At risk 15195	15195	15191	12935	720
Censored 0	0	0	2218	14416
Events 0	0	4	42	59
OnsetNet Q3				
At risk 15129	15127	15108	11916	456
Censored 0	0	0	3132	14572
Events 0	2	21	81	101
OnsetNet Q4				
At risk 15001	15001	14975	10469	250
Censored 0	0	0	4416	14621
Events 0	0	26	116	130

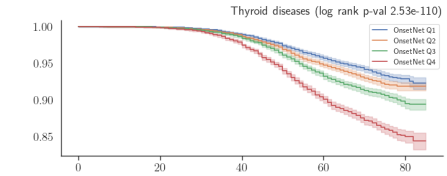

OnsetNet Q1				
At risk 15032	15023	14862	12061	610
Censored 0	0	0	2329	13570
Events 3	12	173	645	855
OnsetNet Q2				
At risk 15117	15096	14909	11982	724
Censored 0	0	0	2351	13371
Events 0	21	208	784	1022
OnsetNet Q3				
At risk 15097	15079	14857	11692	685
Censored 0	0	0	2404	13145
Events 2	20	242	1003	1269
OnsetNet Q4				
At risk 15143	15122	14752	10636	486
Censored 0	0	0	3035	12846
Events 2	23	393	1474	1813

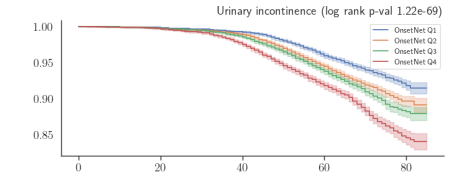

OnsetNet Q1				
At risk 15064	15041	14949	13481	749
Censored 0	0	0	979	13369
Events 1	24	116	605	947
OnsetNet Q2				
At risk 15076	15039	14906	12731	565
Censored 0	0	0	1515	13304
Events 1	38	171	831	1208
OnsetNet Q3				
At risk 15079	15039	14855	11585	536
Censored 0	0	0	2570	13261
Events 0	40	224	924	1282
OnsetNet Q4				
At risk 15175	15126	14794	8957	605
Censored 0	0	0	5014	13013
Events 0	49	381	1204	1557

Fig. C14: Kaplan-Meier curves plotting survival probability (vertical) against age in years (horizontal). (8/9)

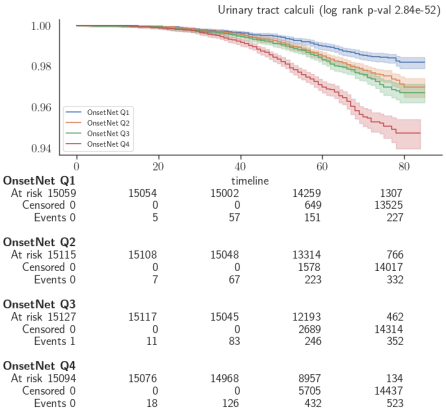

Fig. C15: Kaplan-Meier curves plotting survival probability (vertical) against age in years (horizontal). (9/9)

C.4 Inter-disease risk analysis

C.4.1 Onset acceleration correlation

The clustering dendrogram in Figure 5 utilized UPGMA (unweighted pair group method with arithmetic mean) hierarchical agglomerative clustering for the linkage function (SciPy *cluster.hierarchy.linkage*) with cosine distance between correlation vectors as the clustering metric, where $d(u, v) = \sum_{i,j} \frac{c(u[i],v[j])}{(|u||v|)}$ defined the linkage function between non-identical clusters u and v, i (j) indexes members of cluster u (v), and c denotes cosine distance. Color red (blue) indicates positive (negative)

Fig. C16: All inter-disease Pearson correlations r for non-statin users. Color red (blue) indicates positive (negative) correlation and color intensity scales with correlation magnitude. Conditions with internal test C-index < 0.6 and correlations with $p > 3.46E-5$ (Bonferroni corrected) indicated in gray.

Fig. C17: All inter-disease Pearson correlations r, statin users included. Color red (blue) indicates positive (negative) correlation and color intensity scales with correlation magnitude. Conditions with internal test C-index < 0.6 and correlations with $p > 3.46E - 5$ (Bonferroni corrected) indicated in gray.

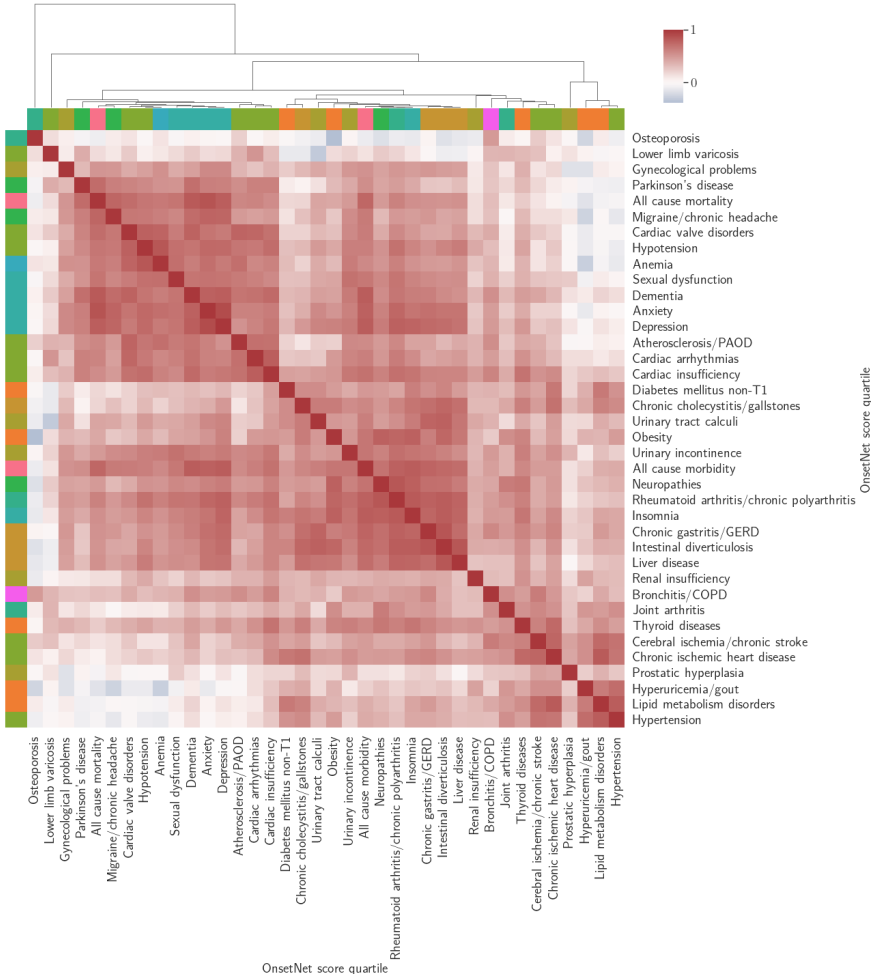

Fig. C18: All-to-all OnsetNet score quartile correlation for conditions with internal test C-index ≥ 0.6, clustered by cosine distance between correlation vectors. Color red (blue) indicates positive (negative) correlation and color intensity scales with correlation magnitude. Statin users were included and 28 out of 1444 entries with $p > 3.46E-5$ (Bonferroni corrected) were set to 0 for cosine distance computation.

Fig. C19: All inter-disease Pearson correlations r for non-statin users without Bonferroni correction. Color red (blue) indicates positive (negative) correlation and color intensity scales with correlation magnitude. Conditions with internal test C-index < 0.6 and correlations with $p > 0.05$ indicated in gray.

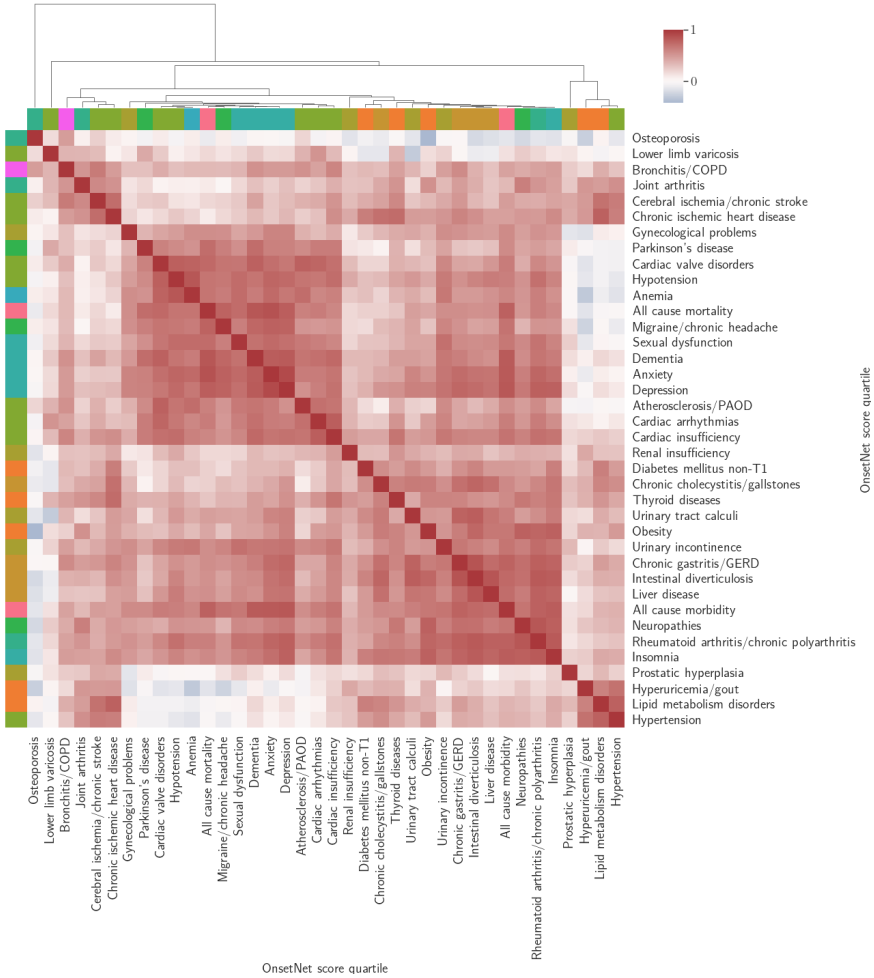

Fig. C20: All-to-all OnsetNet score quartile correlation for non-statin users and conditions with internal test C-index ≥ 0.6, clustered by cosine distance between correlation vectors. Color red (blue) indicates positive (negative) correlation and color intensity scales with correlation magnitude. 12 out of 1444 entries with $p > 0.05$ (no Bonferroni correction) were set to 0 for cosine distance computation.

C.4.2 Associations in onset acceleration correlation

Table C11: Top 5 conditions with highest onset acceleration risk quartile correlation across non-statin users for conditions with internal test C-index ≥ 0.6. All correlations in the top 5 were statistically significant ($p \leq 9.41E-77 \pm 1.29E-75$).

Condition	Top 5 conditions by onset acceleration risk correlation
All cause morbidity	Depression (0.83), anxiety (0.82), dementia (0.82), insomnia (0.81), rheumatoid arthritis/chronic polyarthritis (0.79)
All cause mortality	Anxiety (0.86), dementia (0.84), depression (0.80), all cause morbidity (0.78), migraine/chronic headache (0.77)
Diabetes mellitus non-T1	Chronic ischemic heart disease (0.64), lipid metabolism disorders (0.63), insomnia (0.62), intestinal diverticulosis (0.60), urinary tract calculi (0.56)
Hyperuricemia/ gout	Hypertension (0.70), lipid metabolism disorders (0.61), joint arthritis (0.50), chronic ischemic heart disease (0.50), cerebral ischemia/chronic stroke (0.49)
Lipid metabolism disorders	Chronic ischemic heart disease (0.79), hypertension (0.79), cerebral ischemia/chronic stroke (0.70), diabetes mellitus non-T1 (0.63), hyperuricemia/gout (0.61)
Obesity	Insomnia (0.78), neuropathies (0.78), rheumatoid arthritis/chronic polyarthritis (0.76), intestinal diverticulosis (0.75), liver disease (0.67)
Thyroid diseases	Chronic ischemic heart disease (0.73), cardiac insufficiency (0.68), insomnia (0.67), neuropathies (0.66), rheumatoid arthritis/chronic polyarthritis (0.62)
Chronic cholecystitis/ gallstones	Intestinal diverticulosis (0.76), chronic gastritis/GERD (0.71), liver disease (0.71), chronic ischemic heart disease (0.70), insomnia (0.67)
Chronic gastritis/ GERD	Intestinal diverticulosis (0.85), rheumatoid arthritis/chronic polyarthritis (0.79), all cause morbidity (0.78), urinary tract calculi (0.77), insomnia (0.77)

Table C11 (continued)

Intestinal diverticulosis	Chronic gastritis/GERD (0.85), liver disease (0.84), rheumatoid arthritis/chronic polyarthritis (0.82), insomnia (0.81), urinary tract calculi (0.79)
Liver disease	Intestinal diverticulosis (0.84), rheumatoid arthritis/chronic polyarthritis (0.78), insomnia (0.76), chronic gastritis/GERD (0.73), all cause morbidity (0.72)
Gynecological problems	Anxiety (0.61), depression (0.60), all cause morbidity (0.56), all cause mortality (0.55), anemia (0.55)
Prostatic hyperplasia	Cerebral ischemia/chronic stroke (0.42), chronic ischemic heart disease (0.40), lipid metabolism disorders (0.33), urinary incontinence (0.33), chronic cholecystitis/gallstones (0.31)
Renal insufficiency	Thyroid diseases (0.51), cardiac insufficiency (0.47), hyperuricemia/-gout (0.42), chronic ischemic heart disease (0.42), hypotension (0.41)
Urinary incontinence	Rheumatoid arthritis/chronic polyarthritis (0.73), sexual dysfunction (0.71), depression (0.69), insomnia (0.68), all cause morbidity (0.68)
Urinary tract calculi	Intestinal diverticulosis (0.79), chronic gastritis/GERD (0.77), liver disease (0.68), chronic cholecystitis/gallstones (0.65), insomnia (0.65)
Atherosclerosis/ PAOD	Cardiac valve disorders (0.78), anemia (0.72), cardiac arrhythmias (0.70), cardiac insufficiency (0.69), dementia (0.68)
Cardiac arrhythmias	Cardiac insufficiency (0.80), cardiac valve disorders (0.76), dementia (0.70), atherosclerosis/PAOD (0.70), hypotension (0.67)
Cardiac insufficiency	Cardiac arrhythmias (0.80), dementia (0.75), hypotension (0.73), rheumatoid arthritis/chronic polyarthritis (0.71), cardiac valve disorders (0.71)
Cardiac valve disorders	Hypotension (0.79), atherosclerosis/PAOD (0.78), dementia (0.78), anemia (0.78), cardiac arrhythmias (0.76)

Table C11 (continued)

Cerebral ischemia/ chronic stroke	Chronic ischemic heart disease (0.73), lipid metabolism disorders (0.70), bronchitis/COPD (0.65), hypertension (0.65), thyroid diseases (0.58)
Chronic ischemic heart disease	Lipid metabolism disorders (0.79), thyroid diseases (0.73), cerebral ischemia/chronic stroke (0.73), chronic cholecystitis/gallstones (0.70), diabetes mellitus non-T1 (0.64)
Hypertension	Lipid metabolism disorders (0.79), hyperuricemia/gout (0.70), cerebral ischemia/chronic stroke (0.65), chronic ischemic heart disease (0.63), chronic cholecystitis/gallstones (0.55)
Hypotension	Anemia (0.84), cardiac valve disorders (0.79), anxiety (0.76), depression (0.73), sexual dysfunction (0.73)
Lower limb varicosis	Cardiac arrhythmias (0.52), parkinson's disease (0.41), atherosclerosis/PAOD (0.37), bronchitis/COPD (0.36), thyroid diseases (0.35)
Migraine/ chronic headache	Anxiety (0.78), depression (0.77), all cause mortality (0.77), dementia (0.75), all cause morbidity (0.69)
Neuropathies	Rheumatoid arthritis/chronic polyarthritis (0.84), insomnia (0.79), obesity (0.78), chronic gastritis/GERD (0.71), intestinal diverticulosis (0.71)
Parkinson's disease	Dementia (0.73), all cause mortality (0.72), cardiac arrhythmias (0.64), cardiac insufficiency (0.64), migraine/chronic headache (0.63)
Joint arthritis	Neuropathies (0.63), cerebral ischemia/chronic stroke (0.58), hypertension (0.54), obesity (0.54), chronic ischemic heart disease (0.53)
Osteoporosis	Bronchitis/COPD (0.47), cerebral ischemia/chronic stroke (0.23), atherosclerosis/PAOD (0.19), lower limb varicosis (0.16), chronic ischemic heart disease (0.08)
Rheumatoid arthritis/ chronic polyarthritis	Neuropathies (0.84), insomnia (0.83), intestinal diverticulosis (0.82), chronic gastritis/GERD (0.79), depression (0.79)

Table C11 (continued)

Anxiety	Depression (0.90), all cause mortality (0.86), all cause morbidity (0.82), dementia (0.81), migraine/chronic headache (0.78)
Dementia	All cause mortality (0.84), all cause morbidity (0.82), depression (0.81), anxiety (0.81), cardiac valve disorders (0.78)
Depression	Anxiety (0.90), all cause morbidity (0.83), dementia (0.81), all cause mortality (0.80), rheumatoid arthritis/chronic polyarthritis (0.79)
Insomnia	Rheumatoid arthritis/chronic polyarthritis (0.83), intestinal diverticulosis (0.81), all cause morbidity (0.81), neuropathies (0.79), depression (0.79)
Sexual dysfunction	Anxiety (0.74), all cause mortality (0.73), anemia (0.73), hypotension (0.73), depression (0.71)
Anemia	Hypotension (0.84), cardiac valve disorders (0.78), anxiety (0.74), sexual dysfunction (0.73), atherosclerosis/PAOD (0.72)
Bronchitis/ COPD	Cerebral ischemia/chronic stroke (0.65), cardiac insufficiency (0.60), chronic gastritis/GERD (0.57), dementia (0.54), atherosclerosis/-PAOD (0.54)

C.4.3 Prognostic survival analysis

Prognostic risk evaluation

Although commonly used exclusively for prognostic prediction in biomedical contexts [27], Cox PH models do not assume events must occur after trait measurement baseline. The Cox PH objective function specifies a well-defined optimization problem for risk prediction functions regardless of whether variable x_i (Section 2.3) contains traits of the individual measured before or after the event occurred. Model h_θ^d was trained and evaluated as a general (not exclusively prognostic) risk prediction model taking variable x_i containing imperfect information for event time of condition d whether retrospective or prospective. Prognostic value of the model was separately verified in Section 3.3 with exclusion of events that occurred before trait measurement time.

Fig. C21: All-to-all adjusted log hazard ratios for OnsetNet risk Q4 (Q1 as reference) given primary adjustment with demographic variables. Color red (blue) indicates positive (negative) log hazard ratios and color intensity scales with log hazard ratio magnitude. Results with adjusted hazard ratio $p > 0.05$ (without Bonferroni correction) or Schoenfeld residual $p \leq 0.05$ omitted in gray. Entries that remained statistically significant after secondary adjustment with basic body traits are underlined to denote robustness to change in adjustment.

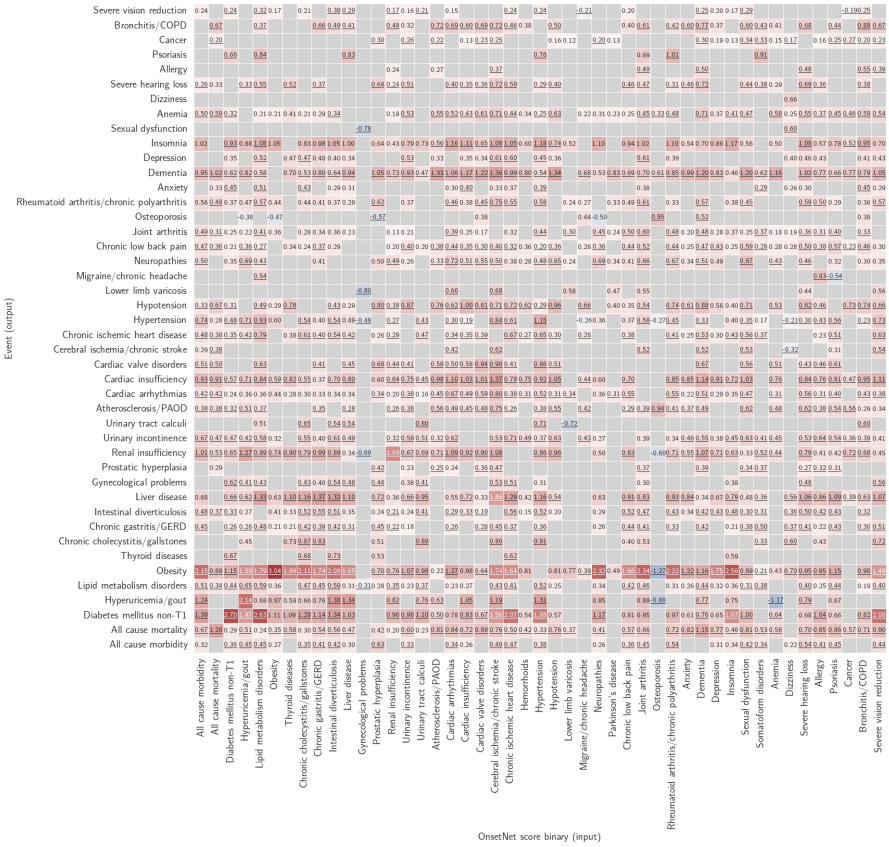

Fig. C22: All-to-all log adjusted hazard ratios for binarized OnsetNet risk (above-median; below-median as reference) given primary adjustment with demographic variables. Color red (blue) indicates positive (negative) log hazard ratios and color intensity scales with log hazard ratio magnitude. Results with adjusted hazard ratio $p > 0.05$ (without Bonferroni correction) or Schoenfeld residual $p \leq 0.05$ omitted in gray. Entries that remained statistically significant after secondary adjustment with basic body traits are underlined to denote robustness to change in adjustment.

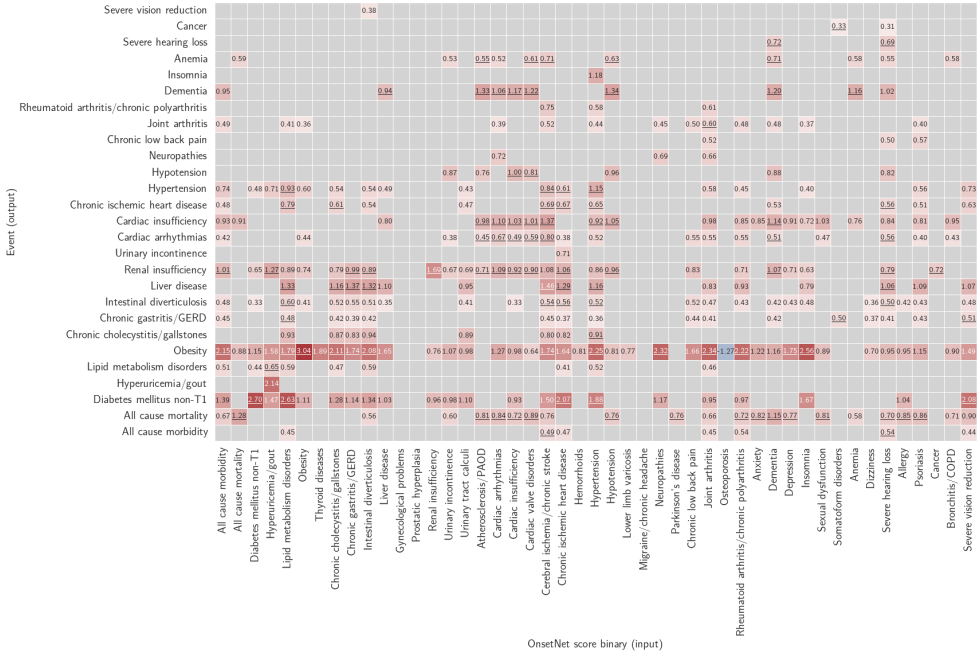

Fig. C23: All-to-all log adjusted hazard ratios for binarized OnsetNet risk (above-median; below-median as reference) given primary adjustment with demographic variables. Color red (blue) indicates positive (negative) log hazard ratios and color intensity scales with log hazard ratio magnitude. Statistically insignificant adjusted hazard ratios with $p > 9.05E-7$ (Bonferroni corrected $p > 0.05$) or Schoenfeld residual $p \leq 0.05$ are omitted in gray. Entries that remained statistically significant after secondary adjustment with basic body traits are underlined to denote robustness to change in adjustment.

C.5 Biomarker saliency

Saliency maps for full traits (demog+bb+bbc+sbc+blood) and full univariate traits (demog+bb+bbc+blood) OnsetNet models are provided.

C.5.1 Full traits model

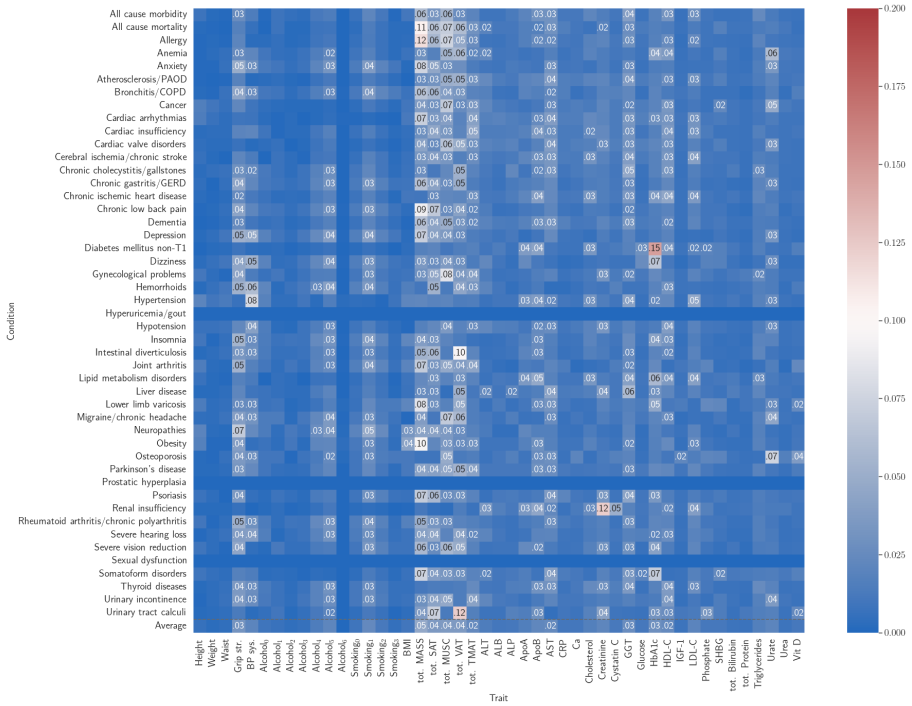

Fig. C24: Univariate saliency for full traits model (female). Top 10 traits for each row are labelled.

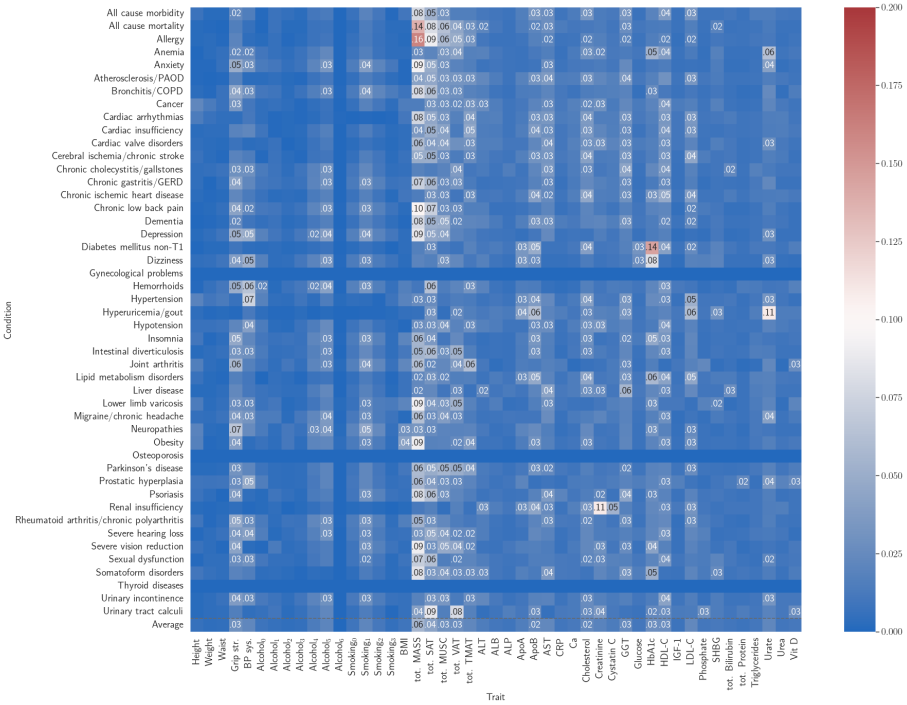

Fig. C25: Univariate saliency for full traits model (male). Top 10 traits for each row are labelled.

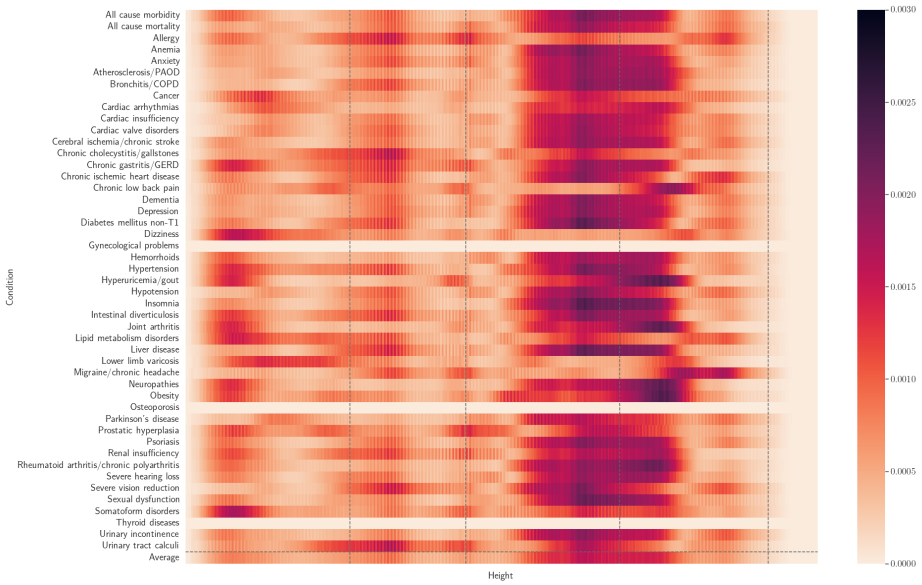

Fig. C26: Spatial body composition saliency across conditions (male MASS).

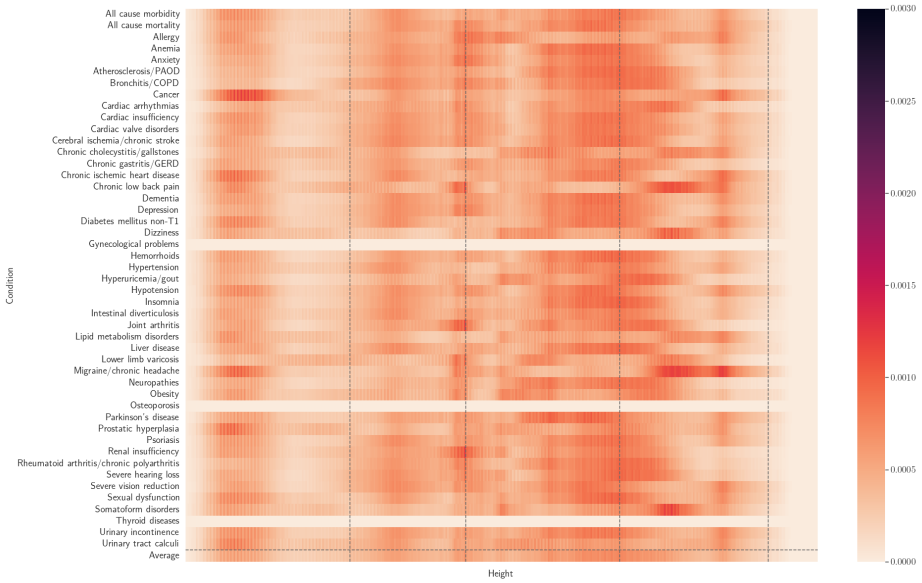

Fig. C27: Spatial body composition saliency across conditions (male MUSC).

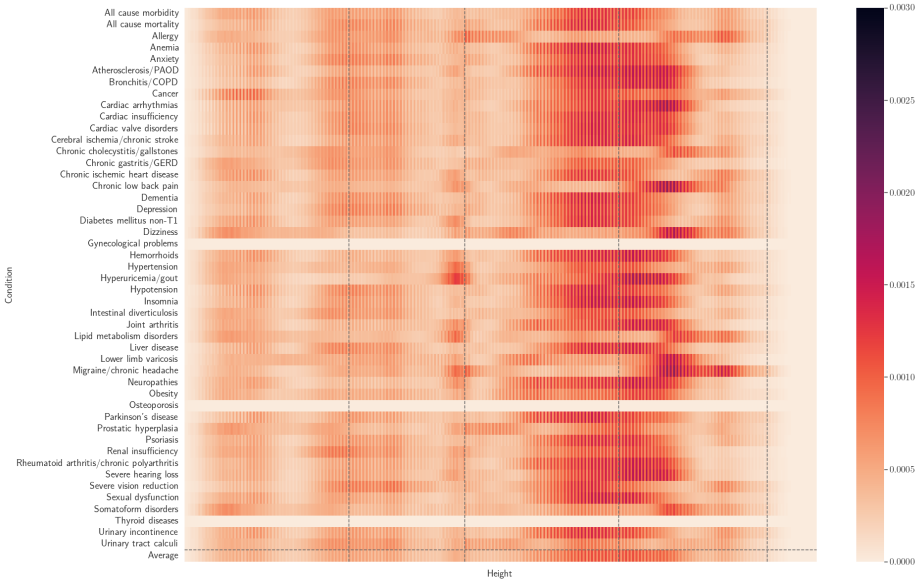

Fig. C28: Spatial body composition saliency across conditions (male SAT).

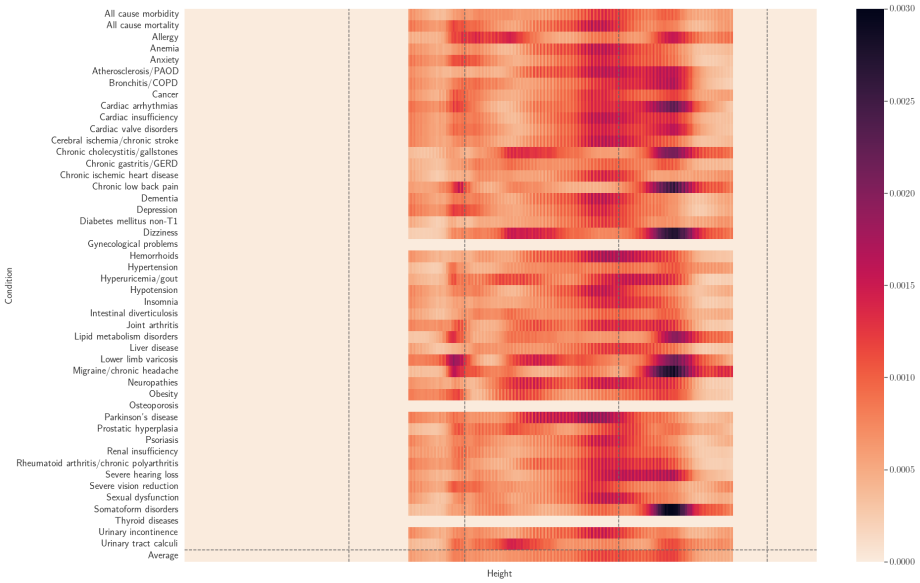

Fig. C29: Spatial body composition saliency across conditions (male VAT).

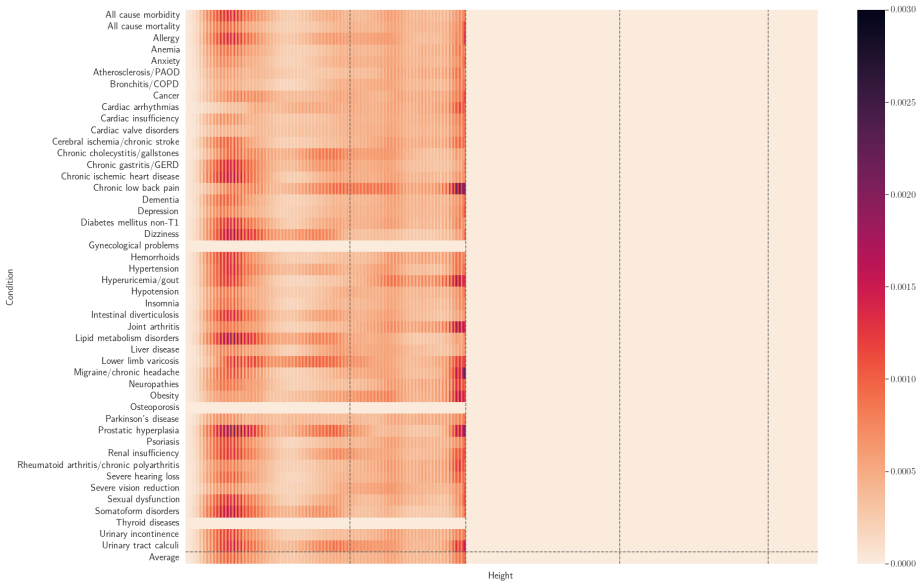

Fig. C30: Spatial body composition saliency across conditions (male TMAT).

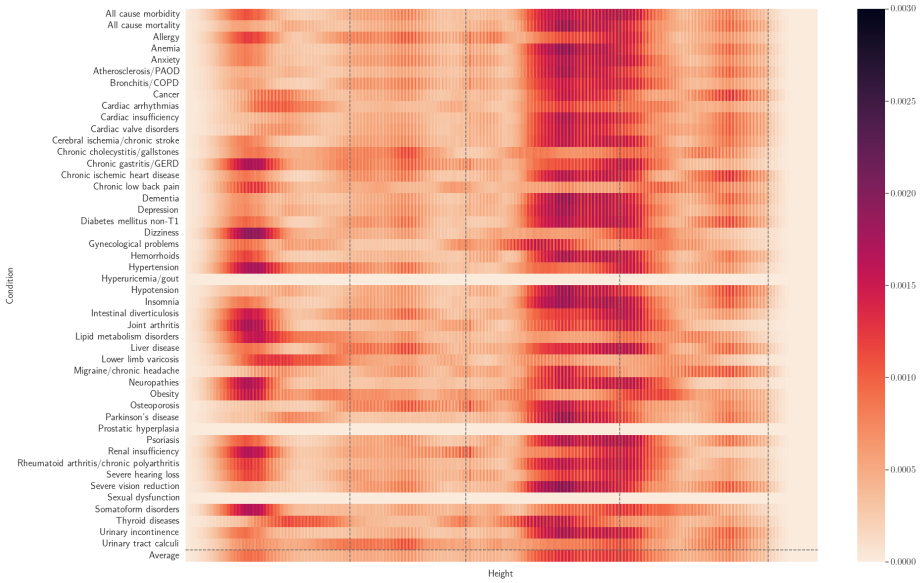

Fig. C31: Spatial body composition saliency across conditions (female MASS).

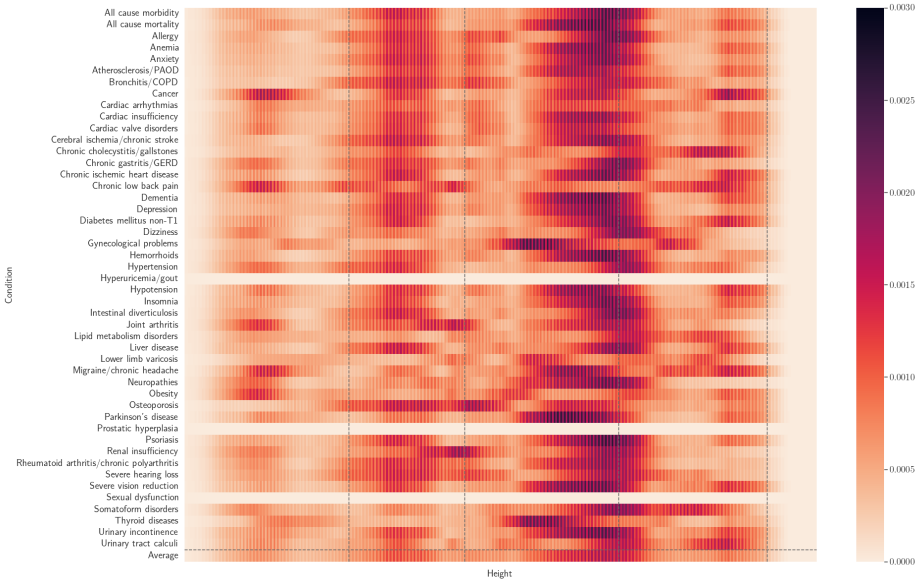

Fig. C32: Spatial body composition saliency across conditions (female MUSC).

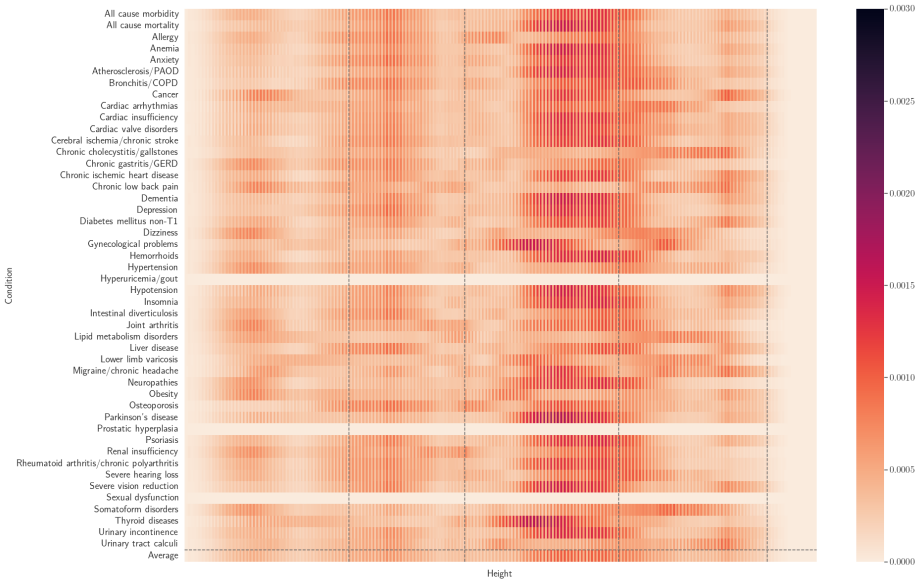

Fig. C33: Spatial body composition saliency across conditions (female SAT).

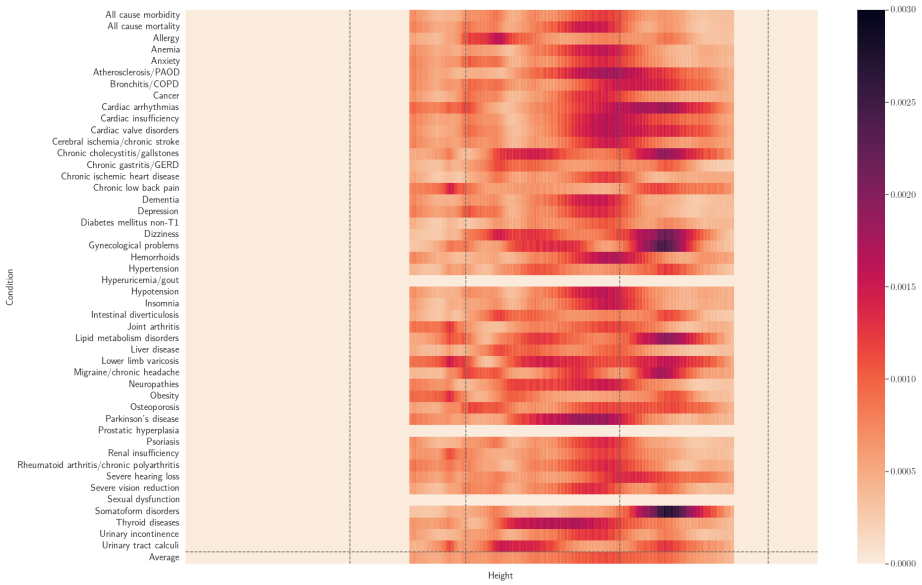

Fig. C34: Spatial body composition saliency across conditions (female VAT).

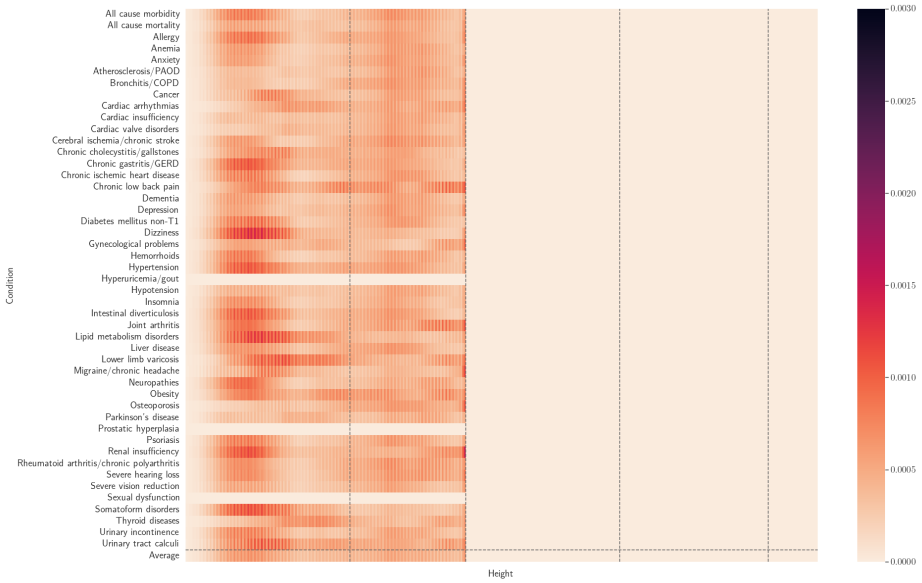

Fig. C35: Spatial body composition saliency across conditions (female TMAT).

C.5.2 Full univariate traits model

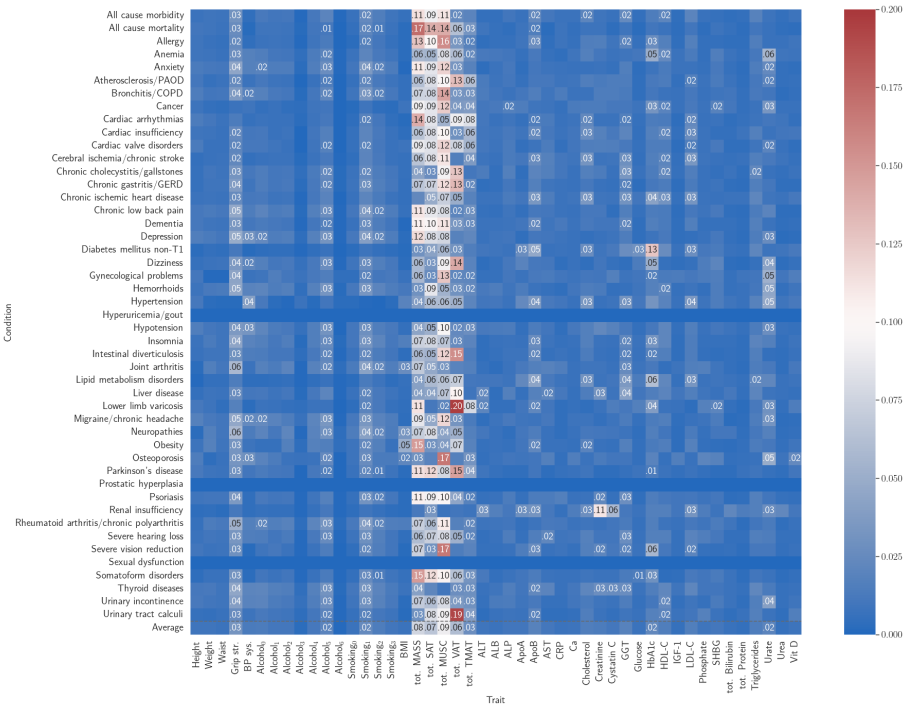

Fig. C36: Univariate saliency for full univariate traits model (female). Top 10 traits for each row are labelled.

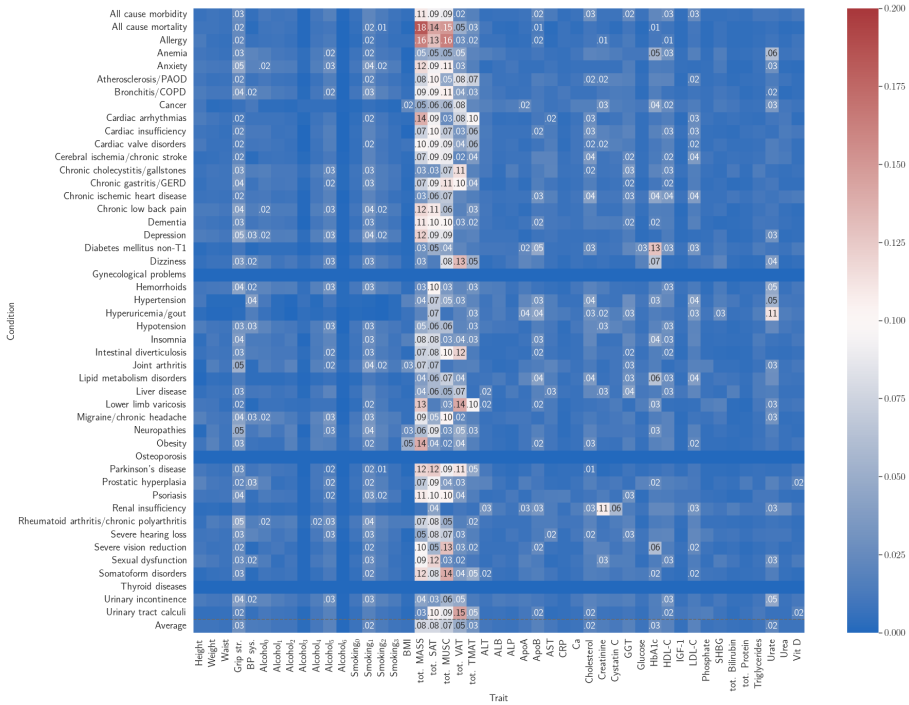

Fig. C37: Univariate saliency for full univariate traits model (male). Top 10 traits for each row are labelled.

Appendix D Reporting checklists

TRIPOD+AI for Abstracts

Section and item	Checklist item
Title	
1 x	Identify the study as developing or evaluating the performance of a multivariable prediction model, the target population, and the outcome to be predicted
Background	
2 x	Provide a brief explanation of the healthcare context and rationale for developing or evaluating the performance of all models
Objectives	
3 x	Specify the study objectives, including whether the study describes model development, evaluation, or both
Methods	
4 x	Describe the sources of data
5 x	Describe the eligibility criteria and setting where the data were collected
6 x	Specify the outcome to be predicted by the model, including time horizon of predictions in case of prognostic models
7 x	Specify the type of model, a summary of the model-building steps, and the method for internal validation†
8 x	Specify the measures used to assess model performance (eg, discrimination, calibration, clinical utility)
Results	
9 x	Report the number of participants and outcome events
10 x	Summarise the predictors in the final model†
11 x	Report model performance estimates (with confidence intervals)
Discussion	
12 x	Give an overall interpretation of the main results
Registration	
13 N/A	Give the registration number and name of the registry or repository

Section/Topic	Item	Development / evaluation[1]	Checklist item	Reported on page
TITLE				
Title	1	D;E	Identify the study as developing or evaluating the performance of a multivariable prediction model, the target population, and the outcome to be predicted	1
ABSTRACT				
Abstract	2	D;E	See TRIPOD+AI for Abstracts checklist	App D
INTRODUCTION				
Background	3a	D;E	Explain the healthcare context (including whether diagnostic or prognostic) and rationale for developing or evaluating the prediction model, including references to existing models	2, 3
	3b	D;E	Describe the target population and the intended purpose of the prediction model in the context of the care pathway, including its intended users (e.g., healthcare professionals, patients, public)	5
	3c	D;E	Describe any known health inequalities between sociodemographic groups	2, 23
Objectives	4	D;E	Specify the study objectives, including whether the study describes the development or validation of a prediction model (or both)	3
METHODS				
Data	5a	D;E	Describe the sources of data separately for the development and evaluation datasets (e.g., randomised trial, cohort, routine care or registry data), the rationale for using these data, and representativeness of the data	5
	5b	D;E	Specify the dates of the collected participant data, including start and end of participant accrual; and, if applicable, end of follow-up	5
Participants	6a	D;E	Specify key elements of the study setting (e.g., primary care, secondary care, general population) including the number and location of centres	5
	6b	D;E	Describe the eligibility criteria for study participants	5, App A
	6c	D;E	Give details of any treatments received, and how they were handled during model development or evaluation, if relevant	N/A
Data preparation	7	D;E	Describe any data pre-processing and quality checking, including whether this was similar across relevant sociodemographic groups	7, App A
Outcome	8a	D;E	Clearly define the outcome that is being predicted and the time horizon, including how and when assessed, the rationale for choosing this outcome, and whether the method of outcome assessment is consistent across sociodemographic groups	7, 8
	8b	D;E	If outcome assessment requires subjective interpretation, describe the qualifications and demographic characteristics of the outcome assessors	N/A
	8c	D;E	Report any actions to blind assessment of the outcome to be predicted	N/A
Predictors	9a	D	Describe the choice of initial predictors (e.g., literature, previous models, all available predictors) and any pre-selection of predictors before model building	5
	9b	D;E	Clearly define all predictors, including how and when they were measured (and any actions to blind assessment of predictors for the outcome and other predictors)	5, 6, App A
	9c	D;E	If predictor measurement requires subjective interpretation, describe the qualifications and demographic characteristics of the predictor assessors	N/A
Sample size	10	D;E	Explain how the study size was arrived at (separately for development and evaluation), and justify that the study size was sufficient to answer the research question. Include details of any sample size calculation	5, App A
Missing data	11	D;E	Describe how missing data were handled. Provide reasons for omitting any data	5, App A
Analytical methods	12a	D	Describe how the data were used (e.g., for development and evaluation of model performance) in the analysis, including whether the data were partitioned, considering any sample size requirements	5, App A
	12b	D	Depending on the type of model, describe how predictors were handled in the analyses (functional form, rescaling, transformation, or any standardisation).	7, App A
	12c	D	Specify the type of model, rationale[2], all model-building steps, including any hyperparameter tuning, and method for internal validation	7, 8
	12d	D;E	Describe if and how any heterogeneity in estimates of model parameter values and model performance was handled and quantified across clusters (e.g., hospitals, countries). See TRIPOD-Cluster for additional considerations[3]	N/A
	12e	D;E	Specify all measures and plots used (and their rationale) to evaluate model performance (e.g., discrimination, calibration, clinical utility) and, if relevant, to compare multiple models	8
	12f	E	Describe any model updating (e.g., recalibration) arising from the model evaluation, either overall or for particular sociodemographic groups or settings	N/A
	12g	E	For model evaluation, describe how the model predictions were calculated (e.g., formula, code, object, application programming interface)	8
Class imbalance	13	D;E	If class imbalance methods were used, state why and how this was done, and any subsequent methods to recalibrate the model or the model predictions	N/A
Fairness	14	D;E	Describe any approaches that were used to address model fairness and their rationale	9, 23
Model output	15	D	Specify the output of the prediction model (e.g., probabilities, classification). Provide details and rationale for any classification and how the thresholds were identified	8, App A

[1] D=items relevant only to the development of a prediction model; E=items relating solely to the evaluation of a prediction model; D;E=items applicable to both the development and evaluation of a prediction model
[2] Separately for all model building approaches.
[3] TRIPOD-Cluster is a checklist of reporting recommendations for studies developing or validating models that explicitly account for clustering or explore heterogeneity in model performance (eg, at different hospitals or centres). Debray et al, BMJ 2023; 380: e071018 [DOI: 10.1136/bmj-2022-071018]

Training versus evaluation	16	D;E	Identify any differences between the development and evaluation data in healthcare setting, eligibility criteria, outcome, and predictors	11, 36
Ethical approval	17	D;E	Name the institutional research board or ethics committee that approved the study and describe the participant-informed consent or the ethics committee waiver of informed consent	25
OPEN SCIENCE				
Funding	18a	D;E	Give the source of funding and the role of the funders for the present study	24
Conflicts of interest	18b	D;E	Declare any conflicts of interest and financial disclosures for all authors	24
Protocol	18c	D;E	Indicate where the study protocol can be accessed or state that a protocol was not prepared	5, 25
Registration	18d	D;E	Provide registration information for the study, including register name and registration number, or state that the study was not registered	5, 25
Data sharing	18e	D;E	Provide details of the availability of the study data	25
Code sharing	18f	D;E	Provide details of the availability of the analytical code[4]	8
PATIENT & PUBLIC INVOLVEMENT				
Patient & Public Involvement	19	D;E	Provide details of any patient and public involvement during the design, conduct, reporting, interpretation, or dissemination of the study or state no involvement.	25
RESULTS				
Participants	20a	D;E	Describe the flow of participants through the study, including the number of participants with and without the outcome and, if applicable, a summary of the follow-up time. A diagram may be helpful.	App A
	20b	D;E	Report the characteristics overall and, where applicable, for each data source or setting, including the key dates, key predictors (including demographics), treatments received, sample size, number of outcome events, follow-up time, and amount of missing data. A table may be helpful. Report any differences across key demographic groups.	11, App A
	20c	E	For model evaluation, show a comparison with the development data of the distribution of important predictors (demographics, predictors, and outcome).	11, App A
Model development	21	D;E	Specify the number of participants and outcome events in each analysis (e.g., for model development, hyperparameter tuning, model evaluation)	11, App A, C
Model specification	22	D	Provide details of the full prediction model (e.g., formula, code, object, application programming interface) to allow predictions in new individuals and to enable third-party evaluation and implementation, including any restrictions to access or re-use (e.g., freely available, proprietary)[5]	8
Model performance	23a	D;E	Report model performance estimates with confidence intervals, including for any key subgroups (e.g., sociodemographic). Consider plots to aid presentation.	13, App C
	23b	D;E	If examined, report results of any heterogeneity in model performance across clusters. See TRIPOD Cluster for additional details[3].	N/A
Model updating	24	E	Report the results from any model updating, including the updated model and subsequent performance	N/A
DISCUSSION				
Interpretation	25	D;E	Give an overall interpretation of the main results, including issues of fairness in the context of the objectives and previous studies	23
Limitations	26	D;E	Discuss any limitations of the study (such as a non-representative sample, sample size, overfitting, missing data) and their effects on any biases, statistical uncertainty, and generalizability	23
Usability of the model in the context of current care	27a	D	Describe how poor quality or unavailable input data (e.g., predictor values) should be assessed and handled when implementing the prediction model	App A
	27b	D	Specify whether users will be required to interact in the handling of the input data or use of the model, and what level of expertise is required of users	N/A
	27c	D;E	Discuss any next steps for future research, with a specific view to applicability and generalizability of the model	4, 5, 23, 24

From: Collins GS, Moons KGM, Dhiman P, et al. *BMJ* 2024;385:e078378. doi:10.1136/bmj-2023-078378

[4] This relates to the analysis code, for example, any data cleaning, feature engineering, model building, evaluation.
[5] This relates to the code to implement the model to get estimates of risk for a new individual.

STROBE Statement—checklist of items that should be included in reports of observational studies

	Item No	Recommendation	
Title and abstract	1	(*a*) Indicate the study's design with a commonly used term in the title or the abstract	X
		(*b*) Provide in the abstract an informative and balanced summary of what was done and what was found	X
Introduction			
Background/rationale	2	Explain the scientific background and rationale for the investigation being reported	X
Objectives	3	State specific objectives, including any prespecified hypotheses	X
Methods			
Study design	4	Present key elements of study design early in the paper	X
Setting	5	Describe the setting, locations, and relevant dates, including periods of recruitment, exposure, follow-up, and data collection	X
Participants	6	(*a*) *Cohort study*—Give the eligibility criteria, and the sources and methods of selection of participants. Describe methods of follow-up *Case-control study*—Give the eligibility criteria, and the sources and methods of case ascertainment and control selection. Give the rationale for the choice of cases and controls *Cross-sectional study*—Give the eligibility criteria, and the sources and methods of selection of participants	X
		(*b*) *Cohort study*—For matched studies, give matching criteria and number of exposed and unexposed *Case-control study*—For matched studies, give matching criteria and the number of controls per case	N/A
Variables	7	Clearly define all outcomes, exposures, predictors, potential confounders, and effect modifiers. Give diagnostic criteria, if applicable	X
Data sources/ measurement	8*	For each variable of interest, give sources of data and details of methods of assessment (measurement). Describe comparability of assessment methods if there is more than one group	X
Bias	9	Describe any efforts to address potential sources of bias	X
Study size	10	Explain how the study size was arrived at	X
Quantitative variables	11	Explain how quantitative variables were handled in the analyses. If applicable, describe which groupings were chosen and why	X
Statistical methods	12	(*a*) Describe all statistical methods, including those used to control for confounding	X
		(*b*) Describe any methods used to examine subgroups and interactions	X
		(*c*) Explain how missing data were addressed	X
		(*d*) *Cohort study*—If applicable, explain how loss to follow-up was addressed *Case-control study*—If applicable, explain how matching of cases and controls was addressed *Cross-sectional study*—If applicable, describe analytical methods taking account of sampling strategy	N/A
		(*e*) Describe any sensitivity analyses	X

Continued on next page

Results			
Participants	13*	(a) Report numbers of individuals at each stage of study—eg numbers potentially eligible, examined for eligibility, confirmed eligible, included in the study, completing follow-up, and analysed	X
		(b) Give reasons for non-participation at each stage	X
		(c) Consider use of a flow diagram	X
Descriptive data	14*	(a) Give characteristics of study participants (eg demographic, clinical, social) and information on exposures and potential confounders	X
		(b) Indicate number of participants with missing data for each variable of interest	X
		(c) *Cohort study*—Summarise follow-up time (eg, average and total amount)	X
Outcome data	15*	*Cohort study*—Report numbers of outcome events or summary measures over time	X
		Case-control study—Report numbers in each exposure category, or summary measures of exposure	
		Cross-sectional study—Report numbers of outcome events or summary measures	
Main results	16	(*a*) Give unadjusted estimates and, if applicable, confounder-adjusted estimates and their precision (eg, 95% confidence interval). Make clear which confounders were adjusted for and why they were included	X
		(*b*) Report category boundaries when continuous variables were categorized	X
		(*c*) If relevant, consider translating estimates of relative risk into absolute risk for a meaningful time period	N/A
Other analyses	17	Report other analyses done—eg analyses of subgroups and interactions, and sensitivity analyses	X
Discussion			
Key results	18	Summarise key results with reference to study objectives	X
Limitations	19	Discuss limitations of the study, taking into account sources of potential bias or imprecision. Discuss both direction and magnitude of any potential bias	X
Interpretation	20	Give a cautious overall interpretation of results considering objectives, limitations, multiplicity of analyses, results from similar studies, and other relevant evidence	X
Generalisability	21	Discuss the generalisability (external validity) of the study results	X
Other information			
Funding	22	Give the source of funding and the role of the funders for the present study and, if applicable, for the original study on which the present article is based	X

*Give information separately for cases and controls in case-control studies and, if applicable, for exposed and unexposed groups in cohort and cross-sectional studies.

Note: An Explanation and Elaboration article discusses each checklist item and gives methodological background and published examples of transparent reporting. The STROBE checklist is best used in conjunction with this article (freely available on the Web sites of PLoS Medicine at http://www.plosmedicine.org/, Annals of Internal Medicine at http://www.annals.org/, and Epidemiology at http://www.epidem.com/). Information on the STROBE Initiative is available at www.strobe-statement.org.